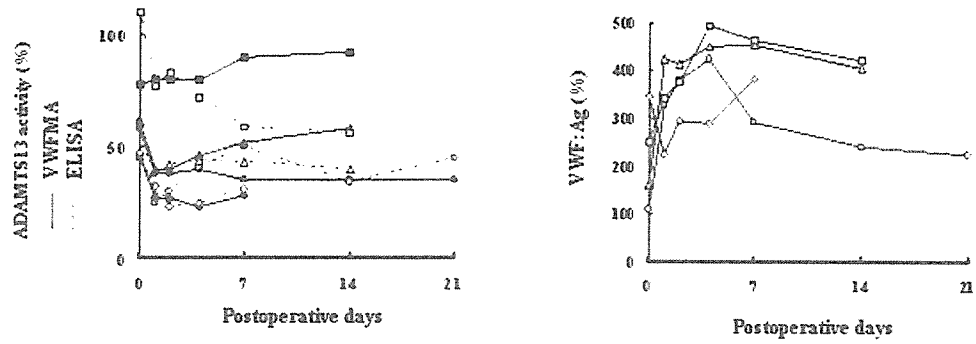

Figure 8. Plasma ADAMTS13 activity (left) and VWF:Ag level (right) after major hepatectomy. Four patients who underwent major hepatectomy were analyzed about ADAMTS13 activity and VWF:Ag for comparison to liver transplantation patients. Circles and triangles show the values of 2 patients who underwent right hepatectomy as living liver donors; Diamonds show a patient with hepatocellular carcinoma who underwent extended right hepatectomy; Squares show a patient with hepatocellular carcinoma who underwent left hepatectomy. Plasma ADAMTS13 activity never decreased below 20%. VWF:Ag levels were rather higher than those in cases 1 to 3 with liver transplantation.

AMTS13 may decrease in the initial phase of adverse events before impairment of graft function.

Interestingly, in case 1, VWF:Ag was markedly increased to 368% and UL-VWFM was detected during the second episode of rejection on day 21, while ADAMTS13 activity was as low as 18% and the platelet count was relatively well maintained at 75,000/μL. These findings indicate that the imbalance of a large amount of UL-VWFM relative to low ADAMTS13 activity could be a good indicator of allograft rejection, even in the absence of severe thrombocytopenia. Thus, our results may be able to explain the fact that liver transplant recipients with increased levels of circulating VWF, a reliable marker of endothelial damage,[40,41] show poor early graft function.[17]

In case 3, ADAMTS13 decreased during hemolysis by B cell-mediated graft-vs.-host disease. However, UL-VWFM was not upregulated during this episode. Differing from ischemia-reperfusion injury or acute rejection, this hemolytic reaction was a systemic reaction due to antibody against blood type A antigen. ADAMTS13, VWF:Ag, and UL-VWFM did not change during nonspecific elevation of ALT around day 25 in case 3. It may be important to analyze ADAMTS13 in combination with UL-VWFM to detect liver transplantation-specific adverse events.

The decrease of ADAMTS13 was milder in patients with major hepatectomy in comparison to liver transplant patients, while VWF:Ag increased higher. This result suggests that significant decrease of ADAMTS13 below 20% would be a liver transplantation-specific event, while the mechanism of difference in changes of ADAMTS13 activity between hepatectomy and liver transplantation is unknown.

The primary target of ischemia-reperfusion injury and allograft rejection is the sinusoidal endothelial cells of the liver graft.[24-26,42] Deposition of activated platelets on the sinusoidal endothelium with a concomitant increase of VWF expression have been found in the liver immediately after reperfusion or cold preservation.[24,25] In addition, upregulated VWF expression has been observed in liver allografts during acute rejection.[25] Furthermore, recipients with acute rejection show enhanced cytokinemia including tumor necrosis factor-α, which leads to endothelial activation and stimulates the release of UL-VWFM from endothelial cells.[38,42] VWF, the substrate of ADAMTS13, synthesized in vascular endothelial cells, mediates the initiation and progression of thrombus formation at sites of vascular injury.[14,40,41,43] VWF is released into plasma as UL-VWFM, which has high platelet aggregation activity. The deficiency of ADAMTS13, together with the excessive release of UL-VWFM from injured graft endothelial cells observed in our study, may cause sinusoidal microcirculatory disturbance and subsequent graft dysfunction.

Various degrees of thrombocytopenia were commonly observed after liver transplantation, especially during the first postoperative week, and many of these patients recover without specific treatment. However, it might be possible that thrombocytopenia is a sign of deterioration of the liver graft in some of the patients with thrombocytopenia, because clinical studies demonstrated that thrombocytopenia was associated with poor prognosis.[22-25,27] If thrombocytopenia is combined with significant decrease of ADMTS13, liver graft function may be deteriorated via the TTP like mechanism due to microcirculatory disturbance. Therefore, monitoring of ADAMTS13 would be quite important to judge the necessity of treatment for thrombocytopenia. In case 1, we administered a large amount of FFP from day 7 to prevent further deterioration of thrombocytopenia with TMA mechanism. In cases 2 and 3, a limited dose of FFP was administered as a prophylaxis of graft dysfunction due to TMA-like reaction, because the ADAMTS13 activity significantly decreased. However, it is to be elucidated whether such prophylactic use of FFP based on the ADAMTS13 activity would provide a beneficial effect.

The values of decreased plasma ADAMTS13 activity by VWF-multimer assay in the present study do not appear to be influenced by the elevated plasma UL-VWFM, because the comparable results are drawn by the novel enzyme-linked immunosorbent assay, which is totally insensitive to the presence of intact VWFM.[29]

This new enzyme-linked immunosorbent assay method would be very useful in clinical application of ADAMTS13 monitoring in liver transplantation, because the results can be obtained within several hours.

At present, FFP is the only available source of ADAMTS13 replacement.[18] Remarkably, in our patients, infusion of FFP, but not platelet concentrate, resulted in gradual improvement of severe thrombocytopenia together with an increase in ADAMTS13 activity. This is an extremely important issue in the treatment of thrombocytopenia associated with allograft dysfunction after liver transplantation, because administration of platelet concentrate under pathological conditions, including an imbalance between decreased ADAMTS13 activity and enhanced VWF production, would further exacerbate the formation of platelet aggregates mediated by uncleaved UL-VWFM, leading to multiorgan failure, as seen in TMA.[2] Platelet concentrate was never administered in case 3 even when the platelet count decreased to 13,000/μL on days 4 to 6, because the activity of ADAMTS13 was low. The mechanism of thrombocytopenia associated with early adverse events after liver transplantation is noteworthy. In the post-transplantation period, patients are especially susceptible to TMA because of administration of calcineurin inhibitors including tacrolimus and cyclosporine, which are well-documented to induce TMA.[44] In case 1, we successfully treated the thrombocytopenia by administering high-dose FFP without conversion of calcineurin inhibitors. Therefore, it would be particularly useful to determine the values of ADAMTS13 and its substrate, VWF:Ag, together with UL-VWFM in the early period after transplantation, not only for the diagnosis of TMA, but also for clarifying the mechanism of thrombocytopenia. Our experience, although based on only 3 liver transplantations and 4 major hepatectomy cases, may provide useful data that are relevant to the diagnosis and treatment of ischemia-reperfusion injury and allograft rejection, as well as for clarifying the pathogenesis of thrombocytopenia after liver transplantation.

REFERENCES

1. Walkentin TE, Kelton JG. Acquired platelet disorders. In: Bloom AL, Forbes CD, Thomas TP, Tuddenham EGD, eds. Hemostasis and Thrombosis. London: Churchill-Livingstone, 1994:767-815.
2. Moake JL. Thrombotic microangiopathies. N Engl J Med 2002;347:589-599.
3. Pham PT, Danovitch GM, Wilkinson AH, Gritsch HA, Pham PC, Eric TM, et al. Inhibitors of ADAMTS13: a potential factor in the cause of thrombotic microangiopathy in a renal allograft recipient. Transplantation 2002;74:1077-1080.
4. Nakazawa Y, Hashikura Y, Urata K, Ikegami T, Terada M, Yagi H, et al. Von Willebrand factor-cleaving protease activity in thrombotic microangiopathy after living donor liver transplantation: a case report. Liver Transpl 2003;9:1328-1333.
5. Trimarchi HM, Truong LD, Brennan S, Gonzalez JM, Suki WN. FK506-associated thrombotic microangiopathy: report of two cases and review of the literature. Transplantation 1999;67:539-544.
6. Ramasubbu K, Mullick T, Koo A, Hussein M, Henderson JM, Mullen KD, Avery RK. Thrombotic microangiopathy and cytomegalovirus in liver transplant recipients: a case-based review. Transpl Infect Dis 2003;5:98-103.
7. Sekido H, Matsuo K, Takeda K, Morioka D, Kubota T, Tanaka K, et al. Successful adult ABO-incompatible liver transplantation: therapeutic strategy for thrombotic microangiopathy is the key to success. Transplantation 2003;75:1605-1607.
8. Humar A, Jessurun J, Sharp HL, Gruessner RW. Thrombotic microangiopathy after liver-small bowel transplant. Clin Transplant 1998;12:600-601.
9. Burke GW, Ciancio G, Cirocco R, Markou M, Roth D, Esquenazi V, et al. Tacrolimus-related microangiopathy in kidney and simultaneous pancreas-kidney recipients: evidence of endothelin and cytokine involvement. Transplant Proc 1998;30:661-662.
10. Uemura M, Tatsumi K, Matsumoto M, Fujimoto M, Matsuyama T, Ishikawa M, et al. Localization of ADAMTS13 to the stellate cells of human liver. Blood 2005;106:922-924.
11. Soejima K, Mimura N, Hirashima M, Maeda H, Hamamoto T, Nakagaki T, Nozaki C. A novel human metalloprotease synthesized in the liver and secreted into the blood: Possibly, the von Willebrand factor-cleaving protease? J Biochem 2001;130:475-480.
12. Levy GG, Nichols WC, Lian EC, Foroud T, McClintick JN, McGee BM, et al. Mutations in a member of the ADAMTS gene family cause thrombotic thrombocytopenic purpura. Nature 2001;413:488-480.
13. Zheng X, Chung D, Takayama TK, Majerus EM, Sadler JE, Fujikawa K. Structure of von Willebrand factor-cleaving protease (ADAMTS 13), metalloproteinase involved in thrombotic thrombocytopenic purpura. J Biol Chem 2001;276:41089-41163.
14. Plaimauer B, Zimmermann K, Volkel D, Antoine G, Kerschbaumer R, Jenab P, et al. Cloning, expression and characterization of the von Willebrand factor-cleaving protease (ADAMTS 13). Blood 2002;100:3626-3632.
15. Ruggeri ZM. Von Willebrand factor, platelets and endothelial cell interactions. J Thromb Haemost 2003;1:1335-1342.
16. Furlan M, Robles R, Galbusera M, Remuzzi G, Kyrle PA, Brenner B, et al. von Willebrand factor-cleaving protease in thrombotic thrombocytopenic purpura and the hemolytic-uremic syndrome. New Engl J Med 1998;339:1578-1584.
17. Tsai H-M, Lian ECY. Antibody to von Willebrand factor-cleaving protease in acute thrombotic thrombocytopenic purpura. N Engl J Med 1998;339:1585-1594.
18. Mori Y, Wada H, Gabazza EC, Minami N, Nobori T, Shiku H, et al. Predicting response to plasma exchange in patients with thrombotic thrombocytopenic purpura with measurement of vWF-cleaving protease activity. Transfusion 2002;42:572-580.
19. McCaughan GW, Herkes R, Powers B, Rickard K, Gallagher ND, Thompson JF, Sheil AG. Thrombocytopenia post liver transplantation. Correlations with pre-operative platelet count, blood transfusion requirements, allograft function and outcome. J Hepatol 1992;16:16-22.
20. Randoux O, Gambiez L, Navarro F, Declerck N, Labalette M, Dessaint JP, Pruvot FR. Post-liver transplantation thrombocytopenia: a persistent immunologic sequestration? Transplant Proc 1995;27:1710-1711.
21. Richards EM, Alexander GJ, Calne RY, Baglin TP. Thrombocytopenia following liver transplantation is associated with platelet consumption and thrombin generation. Br J Haematol 1997;98:315-321.
22. Chatzipetrou MA, Tsaroucha AK, Weppler D, Pappas PA, Kenyon NS, Nery JR, et al. Thrombocytopenia after liver transplantation. Transplantation 1999;67:702-706.

23. Ben Hamida C, Lauzet JY, Rezaiguia-Delclaux S, Duvoux C, Cherqui D, Duvaldestin P, Stephan F. Effect of severe thrombocytopenia on patient outcome after liver transplantation. Intensive Care Med 2003;29:756-762.
24. Kiuchi K, Oldhafer KJ, Schlitt HJ, Nashan B, Deiwick A, Wonigeit K, et al. Background and prognostic implications of perireperfusion tissue injuries in human liver transplants: a panel histochemical study. Transplantation 1998;66:737-747.
25. Jassem W, Koo DD, Cerundolo L, Rela M, Heaton ND, Fuggle SV. Cadaveric versus living-donor livers: differences in inflammatory markers after transplantation. Transplantation 2003;76:1599-1603.
26. Upadhya GA, Strasberg SM. Platelet adherence to isolated rat hepatic sinusoidal endothelial cells after cold preservation. Transplantation 2002;73:1764-1770.
27. Basile J, Busuttil A, Sheiner PA, Emre S, Guy S, Schwartz ME, et al. Correlation between von Willebrand factor levels and early graft function in clinical liver transplantation. Clin Transplant 1999;13:25-31.
28. Furlan M, Robles R, Solenthaler M, Wassmer M, Sandoz P, Lammle B. Deficiency activity of von Willebrand factor-cleaving protease in chronic relapsing thrombotic thrombocytopenic purpura. Blood 1997;89:3097-3103.
29. Kato S, Matsumoto M, Matsuyama T, Hiura H, Fujimura Y. Monoclonal antibodies to a VWF-A2 decapeptide with the C-terminal residue Tyr1605, generated by ADAMTS13 cleavage, develops a highly sensitive ELISA for its activity and characterize Upshaw-Schulman syndrome. Blood 2005;106(Abs# 2643).
30. Kokame K, Matsumoto M, Fujimura Y, Miyata T. VWF73, a region from D1596 to R1668 of von Willebrand factor, provides a minimal substrate for ADAMTS-13. Blood 2005;103:607-612.
31. Warren CM, Krzesinski PR, Greaser ML. Vertical agarose gel electrophoresis and electroblotting of high molecular-weight proteins. Electrophoresis 2003;24:1695-1702.
32. Marzano A, Gaia S, Ghisetti V, Carenzi S, Premoli A, Debernardi-Venon W, et al. Viral load at the time of liver transplantation and risk of hepatitis B virus recurrence. Liver Transpl 2005;11:402-409.
33. Porte RJ, Blauw E, Knot EA, de Maat MP, de Ruiter C, Minke Bakker C, Terpstra OT. Role of the donor liver in the origin of platelet disorders and hyperfibrinolysis in liver transplantation. J Hepatol 1994;21:592-600.
34. Martin TG 3rd, Somberg KA, Meng YG, Cohen RL, Heid CA, de Sauvage FJ, Shuman MA. Thrombopoietin levels in patients with cirrhosis before and after orthotopic liver transplantation. Ann Intern Med 1997;127:285-288.
35. Moake JL, Rudy CK, Troll JH, Weinstein MJ, Colannino NM, Azocar J, et al. Unusually large plasma factor VIII: von Willebrand factor multimers in chronic relapsing thrombotic thrombocytopenic purpura. N Engl J Med 1982;307:1432-1435.
36. Knittel T, Neubauer K, Armbrust T, Ramadori G. Expression of von Willebrand factor in normal and diseased rat livers and in cultivated liver cells. Hepatology 1995;21:470-476.
37. Urashima S, Tsutsumi M, Nakase K, Wang JS, Takada A. Studies on capillarization of the hepatic sinusoids in alcoholic liver disease. Alcohol Alcohol 1993;28:77-84.
38. Bernardo A, Ball C, Nolasco L, Moake JF, Dong J. Effects of inflammatory cytokines on the release and cleavage of the endothelial cell-derived ultralarge von Willebrand factor multimers under flow. Blood 2004;104:100-106.
39. Maring JK, Klompmaker IJ, Zwaveling JH, van Der Meer J, Limburg PC, Slooff MJ. Endotoxins and cytokines during liver transplantation: changes in plasma levels and effects on clinical outcome. Liver Transpl 2000;6:480-488.
40. Stel HV, van der Kwast TH, Veerman EC. Detection of factor VIII/coagulant antigen in human liver tissue. Nature 1983;303:530-532.
41. Baruch Y, Neubauer K, Ritzel A, Wilfling T, Lorf T, Ramadori G. Von Willebrand gene expression in damaged human liver. Hepatogastroenterology 2004;51:684-688.
42. Hoffmann MW, Wonigeit K, Steinhoff G, Herzbeck H, Flad HD, Pichlmayr R. Production of cytokines (TNF-alpha, IL-1-beta) and endothelial cell activation in human liver allograft rejection. Transplantation 1993;55:329-335.
43. Pimanda JE, Ganderton T, Maekawa A, Yap CL, Lawler J, Kershaw G, et al. Role of thrombospondin-1 in control of von Willebrand factor multimer size in mice. J Biol Chem 2004;279:21439-21448.
44. Tamura S, Sugawara Y, Matsui Y, Kishi Y, Akamatsu N, Kaneko J, Makuuchi M. Thrombotic microangiopathy in living-donor liver transplantation. Transplantation 2005;80:169-175.

Novel monoclonal antibody-based enzyme immunoassay for determining plasma levels of ADAMTS13 activity

Seiji Kato, Masanori Matsumoto, Tomomi Matsuyama, Ayami Isonishi, Hisahide Hiura, and Yoshihiro Fujimura

BACKGROUND: ADAMTS13 specifically cleaves unusually large von Willebrand factor (VWF) multimers, which induce platelet thrombi formation under high shear stress. ADAMTS13 activity is deficient in patients with thrombotic thrombocytopenic purpura (TTP). The determination of plasma levels of ADAMTS13 activity is a prerequisite for a differential diagnosis of thrombotic microangiopathies. Here, a unique and highly sensitive enzyme immunoassay (EIA) of ADAMTS13 activity is described.

STUDY DESIGN AND METHODS: ADAMTS13 hydrolyzes the peptide bond between Y1605 and M1606 of VWF. In this assay, a recombinant fusion protein (GST-VWF73-His) is used as a substrate. A panel of mouse monoclonal antibodies (MoAbs) that specifically recognizes Y1605, which is the C-terminal edge residue of the VWF-A2 domain and is generated by the enzymatic cleavage, has been produced. These antibodies were prepared with a synthetic decapeptide, termed N-10 (1596-DREQAPNLVY-1605), as the immunogen. Twenty-six clones specific to N10 were obtained, and one anti-N10 MoAb was used in this study.

RESULTS: With horseradish peroxidase–conjugated anti-N10 MoAb, a standard enzyme assay was established. This assay was highly sensitive, and the detection limit was 0.5 percent of the normal. Further, an inhibitor of ADAMTS13 was measured to a level of 0.1 Bethesda units per mL. ADAMTS13 activity was measured in 20 patients with Upshaw-Schulman syndrome, a congenital TTP, and 61 acquired TTP patients. The activity measured by this assay and by the classic VWF multimer assay showed high correlation.

CONCLUSION: A convenient and highly sensitive EIA for ADAMTS13 activity has been established. This assay can be introduced for routine laboratory work in transfusion medicine.

Thrombotic thrombocytopenic purpura (TTP) is a life-threatening disorder characterized by Moschcowitz's pentad of thrombocytopenia, microangiopathic hemolytic anemia, fluctuating neurologic signs, renal impairment, and fever.[1] With the exception of the thrombocytopenia, however, recent studies have indicated that clinical features of TTP are highly heterogeneous.[2,3] This observation has become solid after a discovery of von Willebrand factor (VWF)-cleaving protease or ADAMTS13 (a disintegrin-like and metalloproteinase with thrombospondin type 1 motif 13).[4-9] A laboratory diagnosis of TTP is now made upon measurement of plasma ADAMTS13 activity,[10,11] congenitally conferred by mutations in the ADAMTS13 gene in Upshaw-Schulman syndrome (USS)[12] or acquired after the development of neutralizing and/or nonneutralizing autoantibodies.

ADAMTS13 is primarily produced by the stellate cells of liver (Itoh cells) and then thought to be released into circulation via the microsinusoidal system.[13] Under the physiologically high shear stresses of this site, ADAMTS13

ABBREVIATIONS: BU(s) = Bethesda unit(s); GST = glutathione *S*-transferase; His = histidine; TMA(s) = thrombotic microangiopathy(-ies); TTP = thrombotic thrombocytopenic purpura; USS = Upshaw-Schulman syndrome; WB(s) = Western blot(s).

From the Department of Blood Transfusion Medicine, Nara Medical University, Nara; and the Research Institute of Japan Clinical Laboratory, Kyoto, Japan.

Address reprint requests to: Yoshihiro Fujimura, MD, Department of Blood Transfusion Medicine, Nara Medical University, 840 Shijo-cho, Kashihara City, Nara, 634-8522, Japan; e-mail: yfujimur@naramed-u.ac.jp.

This work was supported in part by research grants from the Japanese Ministry of Education, Culture, and Science (to Y.F. and M.M.) and the Ministry of Health and Welfare of Japan for Blood Coagulation Abnormalities H17-02 (to Y.F.).

Received for publication November 18, 2005; revision received January 16, 2006, and accepted January 22, 2006.

doi: 10.1111/j.1537-2995.2006.00914.x

TRANSFUSION 2006;46:1444-1452.

specifically cleaves the Y1605-M1606 bond of the VWF-A2 domain. Deficiency of this enzyme results in the accumulation of unusually large VWF multimers in the circulation that can lead to platelet (PLT) aggregation.[14]

During the past decade, assessment of plasma ADAMTS13 activity was performed by an electrophoretic technique with purified VWF as a substrate. This method required a relatively long reaction time in the presence of protein denaturants, such as 1 to 1.5 mol per L urea or guanidine-HCl.[10,11] More recent studies, however, have used *Escherichia coli*–expressed recombinant VWF-A2 polypeptides, tagged with glutathione *S*-transferase (GST)-histidine (His; GST-VWF73-His) or His-T100 (His-VWF188-T100), as the substrate for ADAMTS13 cleavage in the absence of protein denaturants; these changes have dramatically shortened the reaction time.[15-17] In both the classic and the modern assays, however, the principle for determination of ADAMTS13 activity is based on the quantification of residual undigested substrate. A recently introduced FRETS-VWF73 assay with a fluorogenic substrate,[18] unlike other previously reported assays, directly measures the final product generated by ADAMTS13 cleavage. These assays, however, are not sensitive enough to measure the low levels (approx. 5%) of plasma ADAMTS13 activity. Distinction of these levels is critically important to understand the manifestation of the clinical signs of TTP. In addition, this FRETS-VWF73 assay requires a fluorophotometer, which uncommon in routine diagnostic laboratories.

We have developed a highly sensitive enzyme-linked immunosorbent assay (ELISA) measuring ADAMTS13 activity. First, we prepared specific monoclonal antibodies (MoAbs) directed against the decapeptide of the VWF-A2 domain ending with the C-terminal edge residue Y1605, which is generated by ADAMTS13 cleavage. These MoAbs did not react with intact VWF, but did react with the synthetic decapaptide as well as the monomeric or dimeric N-terminal VWF polypeptide (residues 764-1605). Thus, the peroxidase-labeled MoAb could be used as a detection antibody with recombinant VWF73 (residues 1596-1668 of VWF subunit), tagged with both GST and a His tag (GST-VWF73-His),[15] as the enzyme substrate in this novel ELISA. Because this assay would be completed within 3 hours under the hospital environments, it can be introduced for routine laboratory work in transfusion medicine.

MATERIALS AND METHODS

Assays of ADAMTS13 activity and its inhibitors by VWF multimer analysis

We performed a classic VWF multimer assay to screen plasma samples for ADAMTS13 activity and the presence of inhibitors.[10,12] The detection limit of this method for ADAMTS13 activity was 3 percent of the normal levels. The inhibitor titers are expressed as Bethesda units (BUs),[19] where one inhibitor unit is defined as the amount necessary to reduce ADAMTS13 activity to 50 percent of control levels. A titer of greater than 0.5 BUs per mL was considered to be significant. Before assessing the levels of ADAMTS13 inhibitor, test plasma samples were heat-treated at 56°C for 1 hour to kill endogenous ADAMTS13 activity. After centrifugation, the supernatants were examined by these assays.

Patients and their plasma samples

Patient plasma samples were collected from referring hospitals across Japan, along with the patients' clinical information. Those plasma samples that fulfilled the diagnostic criteria for thrombotic microangiopathies (TMAs)[20] were used in this study. Measurement of plasma ADAMTS13 activities and inhibitor titers by VWF multimer analysis categorized these patients into three groups: 1) less than 3 percent of ADAMTS13 activity without the presence of an inhibitor (congenital TTP or USS), 2) less than 3 percent of ADAMTS13 activity with an inhibitor present (acquired TTP), and 3) moderately decreased (≥3%) or subnormal ADAMTS13 activity with or without its inhibitor (TMA). Patients with the clinical manifestations of constitutive TMA, but with normal ADAMTS13 activity, which might be caused by abnormalities in Factor H or CD46, were excluded from this study.

According to these classifications, 81 patients were examined in this study. Of these, 29 had developed acquired TTP, 32 exhibited TMA with measurable ADAMTS13 activity level, and 20 had USS. ADAMTS13 gene analysis confirmed that all USS patients were either compound heterozygotes or homozygotes for gene abnormalities in this protease. In addition, 33 relatives of these USS patients were identified as the carriers of ADAMTS13 gene mutations.[21-24]

Citrated PLT-poor plasma samples prepared from these subjects were frozen on dry ice, sent to our laboratory, and stored at –80°C until use. Normal citrated plasma samples were obtained from 55 healthy individuals (29 female and 26 male, aged 20-40 years) for use as controls and frozen in aliquots at –80°C. Pooled normal plasma samples from these individuals was used as standard plasma in this study. These studies were conducted with the approval of the ethics committee of Nara Medical University.

Preparation and cleavage of GST-VWF73-His fusion protein

Recombinant GST-VWF73-His fusion protein was expressed in *E. coli* inclusion bodies and purified by the method of Kokame and colleagues.[15] Purified GST-VWF73-His was cleaved with plasma ADAMTS13 by the incubation of 540 ng of substrate with 1 μL of normal plasma in

a total volume of 100 μL of reaction buffer (5 mmol/L Tris-HCl, 10 mmol/L $BaCl_2$, and 1 mmol/L PMSF, pH 5.5) at 37°C for 1 hour. Reactions were terminated by the addition of 1 μL of ethylenediaminetetraacetate (EDTA)-2Na (500 mmol/L).

Production of anti-N10 and N15 murine MoAbs

Two synthetic peptides were designed for use as immunogens in the production of MoAbs, a decapeptide (1596-DREQAPNLVY-1605, termed N10) derived from the VWF-A2 domain and a pentadecapeptide (1596-DREQAPNLVYMVTGN-1610, termed N15). Both peptides were conjugated to keyhole limpet hemocyanin (Asahi Techno Glass Corp., Tokyo, Japan). Four 8-week-old Balb/c mice were immunized subcutaneously with 50 μg of each peptide emulsified in complete Freund's adjuvant (Wako Pure Chemical Industries, Ltd., Osaka, Japan). Three immunizations were performed at 2-week intervals. A final booster was given intraperitoneally at a concentration of 10 μg per 100 μL in saline solution at 2 weeks after the last immunization. Mice splenocytes were fused with myeloma cells (P3U1 cell line) according to the method of Köhler and Milstein.[25] Screening of positive hybridomas was performed by ELISA of culture supernatants in polystyrene microtiter plates coated with the recombinant peptides.

Conjugation of horseradish peroxidase to MoAb

Antibodies were purified from culture supernatants of hybridoma cells with a protein A-Sepharose Fast Flow column (Amersham Bioscience, Corp., Piscataway, NJ). Fractions containing immunoglobulin G (IgG) were pooled and dialyzed against PBS. Purified monoclonal IgG was digested with pepsin; the resulting $F(ab')_2$ fragments were purified by the method of Hamaguchi and associates[26] and conjugated to horseradish peroxidase (HRP).[27]

Western blot analysis

Sodium dodecyl sulfate–polyacrylamide gel electrophoresis (SDS-PAGE) was performed with either a Tris-glycine buffer system[28] or a Tris-tricine buffer system.[29] After electrophoresis, separated proteins were electrophoretically transferred to polyvinylidene fluoride (PVDF) membranes (Bio-Rad, Hercules, CA). After blocking nonspecific binding with 3 percent skim milk, PVDF membranes were incubated with monoclonal IgGs. When indicated, the monoclonal IgGs were labeled with HRP; for unlabeled monoclonal IgGs, bound antibody was detected with peroxidase-labeled anti-mouse IgG. Proteins were visualized by chemiluminescence with Western lightning chemiluminescence reagent (Perkin-Elmer Life Sciences, Inc., Boston, MA) and imaged by X-ray autoradiography (Eastman Kodak, Rochester, NY).

ELISA for ADAMTS13 activity with anti-N10 MoAb

One-hundred microliters of GST-VWF73-His solution (250 ng/mL in PBS with 1 percent BSA) was added to each well of microtiter plates coated with an anti-GST polyclonal antibody (Rockland Immunochemicals, Inc., Gilbertsville, PA) and incubated at 37°C for 1 hour. After three washes with PBS-0.05 percent Tween 20 (PBS/T), 100 μL of each sample, plasma diluted 11-fold in reaction buffer (5 mmol/L acetate buffer and 5 mmol/L $MgCl_2$, pH 5.5) was incubated in the wells at 37°C for 1 hour. After washing the wells three times with PBS/T, 100 μL of HRP-conjugated anti-N10 MoAb (No. 146) was added and incubated at 37°C for 1 hour. Wells were then washed three times with PBS/T. One-hundred microliters of HRP substrate (*o*-phenylendiamine-H_2O_2) was added and incubated for 10 minutes. The reaction was terminated with 100 μL of 1 mol per L H_2SO_4; absorbance was then measured at 492 nm. To generate a reference curve, pooled normal plasma serially diluted in heat-immobilized plasma was assessed. To determine sample activity in plasma, the optical density of the test sample was interpolated against the reference curve. The ADAMTS13 inhibitor titer was measured by the combination of this ELISA with a Bethesda method.

Anti-ADAMTS13 murine MoAb

Two anti-ADAMTS13 murine MoAbs, termed A10 and C7, were produced in our laboratory as previously reported.[13] Of these, A10 completely inhibited plasma ADAMTS13 activity at a final concentration of 50 μg IgG per mL by VWF multimer assay, and the epitope was shown residing on a disintegrin-like domain of ADAMTS13 molecule.[13]

RESULTS

Epitope mapping of anti-N15 and N10 MoAbs

By ELISA-based screening assay, we obtained three MoAb clones specific for peptide N15 and 26 MoAb clones against peptide N10. The reactivity of these MoAbs was also tested by Western blotting (WB) with two GST fusions of VWF, GST-VWF73-His (uncleaved) and GST-VWF10 (cleaved by ADAMTS13; Fig. 1). Clones of anti-N15 MoAbs immunoreacted solely with the intact GST-VWF73-His (35 kDa) and did not react with cleaved GST-VWF10 (30 kDa). In contrast, the clones of anti-N10 MoAbs reacted with the GST-VWF10, but only barely with GST-VWF73-His. We chose two anti-N15 clones (No. 22 and 73) and three anti-N10 clones (No. 116, 146, and 229) for further characterization.

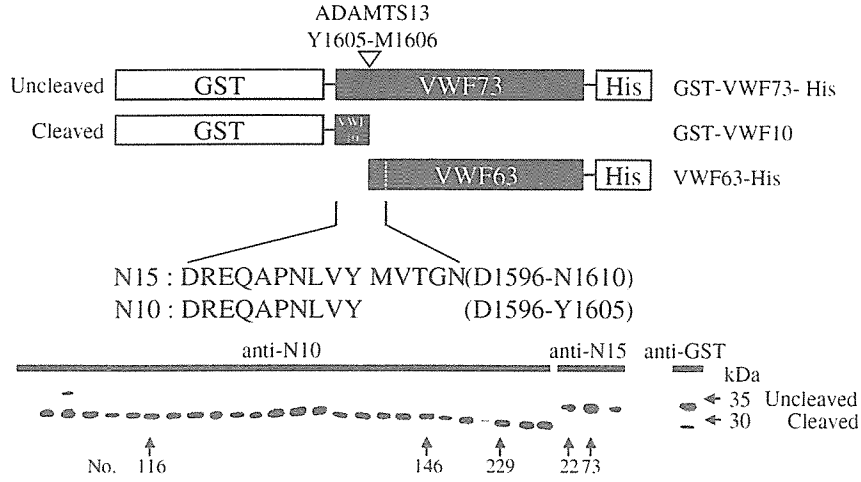

Fig. 1. Production of anti-N10 and anti-N15 murine MoAbs. The schematic structures of the GST-VWF73-His (uncleaved) and GST-VWF10 (cleaved by ADAMTS13) fusions are shown in the top panel. Anti-N10 MoAbs (26 clones), anti-N15 MoAbs (3 clones), and a polyclonal anti-GST antibody serving as a control were used for WB. The anti-N15 clones immunoreacted with the uncleaved GST-VWF73-His band (35 kDa), but not with the cleaved GST-VWF10 (30 kDa). In contrast, the anti-N10 MoAbs reacted with the GST-VWF10, but only minimally with GST-VWF73-His.

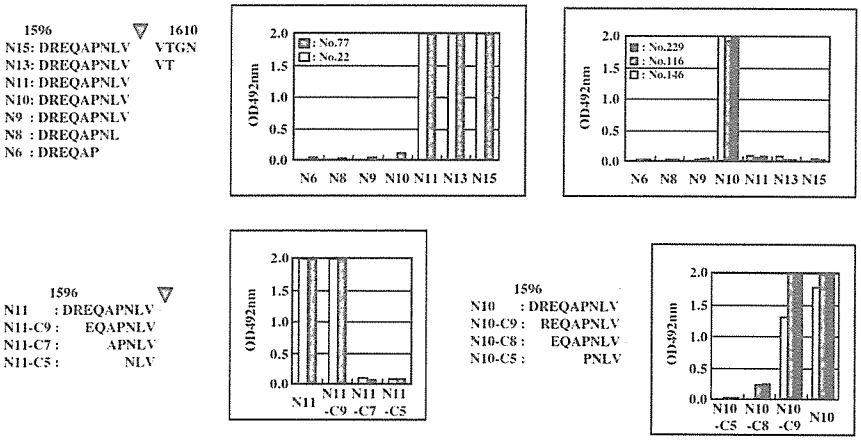

Fig. 2. Epitope mapping of anti-N15 (left) and anti-N10 (right) MoAbs by antigen-immobilized ELISA. For epitope mapping, we tested the immunoreactivities of anti-N15 and anti-N10 MoAbs against a panel of synthetic peptides by ELISA. The immunoreactivities of N15 against the C-terminal truncated peptides are shown in the top panel. The anti-N15 MoAbs reacted with N15 to N11, but lost any interaction upon deletion of M1606. In contrast, the anti-N10 MoAbs specifically reacted with N10 only. In the bottom panel, the reactivity of the anti-N15 and anti-N10 MoAbs with N-terminally deleted N11 and N10 peptides were shown. The anti-N15 MoAbs completely lost their immunoreactivity with the deletion of the four N-terminal residues (D1596 to Q1599) from the N11 peptide. The anti-N10 MoAbs lost their immunoreactivity upon deletion of the two N-terminal residues (D1596 and R1597).

To determine the precise epitopes recognized by these MoAbs, we tested the immunoreactivity of anti-N15 and anti-N10 MoAbs for a panel of synthetic peptides by ELISA (Fig. 2). The two anti-N15 MoAbs shared epitopes within amino acid residues 1596-DREQAPNLVYM-1606 of the VWF-A2 subunit, which required the presence of the two adjacent residues (1605-YM-1606). In contrast, three anti-N10 MoAbs consistently recognized epitopes on the 1597-REQAPNLVY-1605 peptide. For the anti-N10 MoAbs, the presence of Y1605 as the C-terminal residue was an absolute requirement; neither of these MoAbs reacted with the N11 or N9 peptides. Deletion of the two N-terminal residues (D1596 and R1597) from the N10 peptide resulted in an almost complete loss of immunoreactivity with the three anti-N10 MoAb clones. Thus, the epitopes recognized by the anti-N10 MoAbs consistently reside within the 1597-REQAPNLVY-1605 peptide. Hereafter, two MoAbs, one anti-N10 (No. 146) and one anti-N15 (No. 22), were used for further studies.

Immunoreactivity of anti-N15 and anti-N10 MoAbs with VWF fragments generated by ADAMTS13 cleavage

Cleavage of purified VWF by rADAMTS13 generated two major fragments with molecular weights of 340 kDa (C-terminal dimer of VWF subunits of residues 1606-2813) and 280 kDa (N-terminal dimer of VWF subunits of residues 764-1605), analyzed by a SDS-5 percent PAGE under nonreducing conditions. Reducing conditions, however, displayed two distinct bands of 140 kDa (a monomer of VWF residues 764-1605) and 176 kDa (a monomer of VWF residues 1606-2813; Fig. 3). We analyzed these rADAMTS13-cleaved VWF fragments by WB with the anti-N10 and N15 MoAbs.

The anti-N10 MoAb reacted exclusively with the 280-kDa fragment and did not react with the 340-kDa fragment under nonreducing conditions. Under reducing conditions, the anti-N10 MoAb reacted with the 140-kDa fragment, but not with the 176-kDa fragment.

In contrast, the anti-N15 MoAb did not react with VWF either before or after cleavage by rADAMTS13 in either nonreducing or reducing conditions. These results

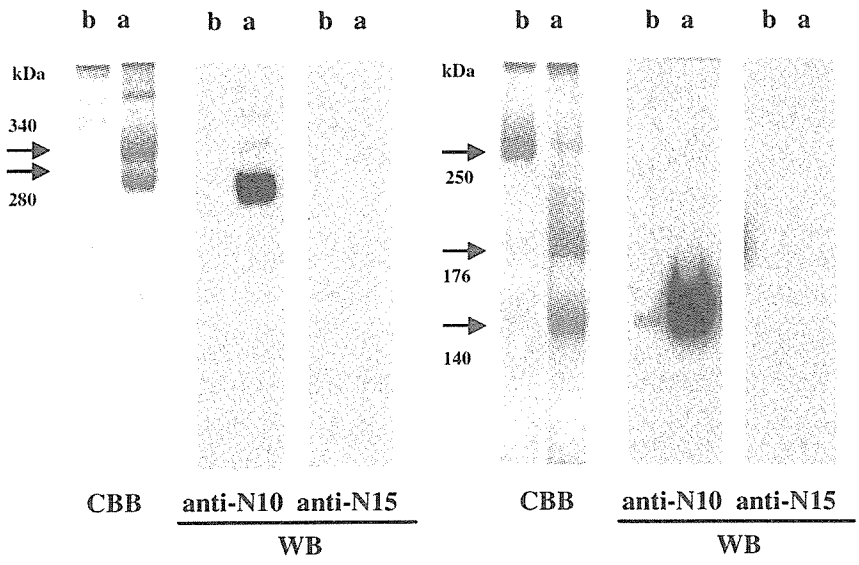

Fig. 3. Immunoreactivity of anti-N10 and anti-N15 MoAbs against VWF fragments generated by ADAMTS13 cleavage. Cleavage of purified VWF by recombinant ADAMTS13 generated two major fragments with molecular weights of 340 kDa (C-terminal dimer of VWF subunit) and 280 kDa (N-terminal dimer of VWF subunit) by a SDS-5 percent PAGE under nonreducing conditions (left). Under reducing conditions (right), two bands corresponding to the N-terminal 140-kDa fragment and the C-terminal 176-kDa fragment could be seen. WB analysis of these VWF fragments before (b) and after (a) cleavage by recombinant ADAMTS13 was performed with the anti-N10 (No. 146) and anti-N15 (No. 22) MoAbs. The anti-N10 MoAb reacted exclusively with the 280-kDa fragment, not the 340-kDa fragment, under nonreducing conditions. Under reducing conditions, the anti-N10 MoAb reacted with the 140-kDa fragment, but not with the 176-kDa fragment or the uncleaved 250-kDa VWF. In contrast, the anti-N15 MoAb did not react with VWF either before or after cleavage by rADAMTS13, under either nonreducing or reducing conditions.

indicate that the epitope recognized by the anti-N15 MoAb on VWF subunit is cryptic before rADAMTS13-mediated cleavage, but no longer exists after cleavage of the 1605-YM-1606 bond. After SDS-1.2 percent agarose gel electrophoresis of normal plasma, WBs with either the anti-N10 or the anti-N15 MoAbs could not detect the VWF multimeric patterns (data not shown).

Establishment of ELISA for ADAMTS13 activity

When ELISA was performed with pooled normal plasma, as described under Materials and Methods, reactivity measured at OD492 nm increased proportionally to the amount of plasma added (Fig. 4A). This additive effect, however, was not seen when with plasma sample derived from patients with USS or acquired TTP. The reactivity of pooled normal plasma was completely blocked by 10 mmol per L EDTA, but was not abolished by the addition of a protease inhibitor cocktail (effective against a broad range of serine proteases, cysteine proteases, aminopeptidases, and acid proteases; Sigma-Aldrich, Inc., St. Louis, MO).

The optimal conditions for this ELISA were determined with pooled normal plasma. We varied the following conditions in the reaction mixture (Fig. 4B): 1) incubation time for enzymatic cleavage, 2) species of divalent metal ions present, 3) NaCl concentration (ionic strength), 4) Mg^{2+} concentration, 5) urea concentration, and 6) pH. The ELISA was most efficient when performed for 1 hour in 5 mmol per L acetate buffer (pH 5.5) containing 5 mmol per L $MgCl_2$ in the absence of urea. A detection limit of 0.5 percent ADAMTS13 activity was estimated by the intersection point of the curve of minus 2.6 standard deviations (SDs) for the standards measured in 10 replications and the zero standards of plus 2.6 SDs (data not shown). To evaluate the precision of this assay, we measured the ADAMTS13 activities present in three different plasma samples in eight replications (within-run assay). The mean ± SD values of three samples were 4.4 ± 0.4, 52.0 ± 2.1, and 103.2 ± 7.4 percent (n = 8). The coefficient of variation values of three samples were 9.7, 3.9, and 7.1 percent (n = 8), respectively (data not shown).

Effect of antibodies in the novel ELISA

Under the optimal conditions determined above, we examined the effect of antibodies against VWF and ADAMTS13 in this novel ELISA (Fig. 5A). Pooled undiluted normal plasma was incubated for 2 hours at 37°C with varying concentrations of each purified IgG; the residual activity of ADAMTS13 in each mixture was then determined. The purified IgG from normal subjects did not exhibit significant inhibition at any concentration tested, but samples from patients with acquired TTP showed a dose-dependent inhibition, completely abrogating ADAMTS13 activity at a final concentration of 500 µg per mL. Anti-ADAMTS13 MoAb A10 (20 µg IgG/mL, final) totally blocked ADAMTS13 activity in this novel ELISA, as shown in the VWF multimer assay. The anti-N15 MoAb displayed total inhibition of plasma ADAMTS13 activity at a concentration of 20 µg per mL. These results indicate that this novel ELISA can specifically recognize the cleavage of the peptide bond between Y1605 and M1606 of the VWF-A2 domain.

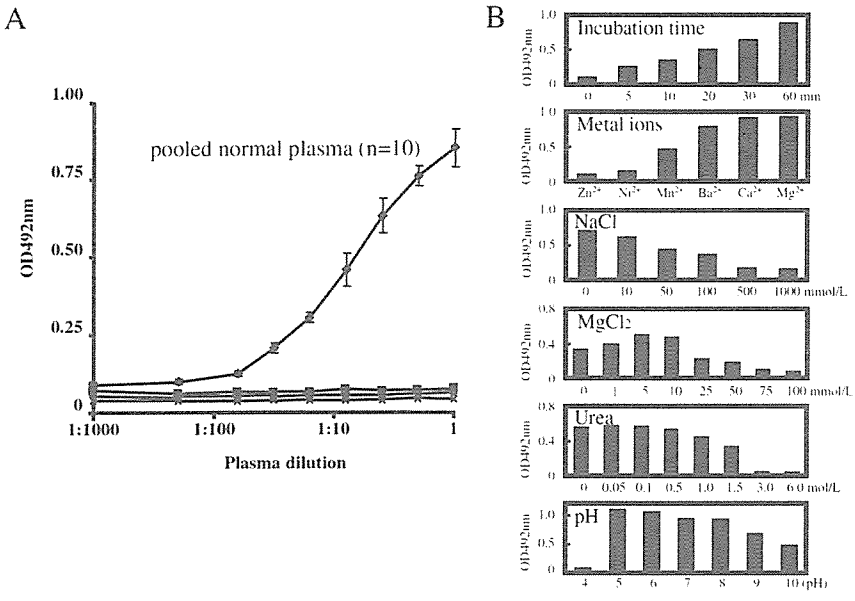

Fig. 4. Establishment of ELISA for ADAMTS13 activity. (A) In this ELISA, intensity at OD492 nm increased in proportion to the normal plasma (◆) concentration. This correlation was not observed for plasma samples from patients with USS (●) or acquired TTP (■) or in the presence of 10 mmol/L EDTA (×). The values for normal plasma shown are the mean and SD (n = 10). (B) Optimal conditions for this ELISA were determined with pooled normal plasma by varying the following conditions: 1) incubation time for enzymatic cleavage, 2) the species of divalent metal ions included (5 mmol/L, final concentration), 3) NaCl concentrations (ionic strength), 4) Mg^{2+} concentrations, 5) urea concentrations, and 6) pH.

Measurement of plasma ADAMTS13 inhibitory activity

We also determined plasma ADAMTS13 inhibitory activity in samples from patients with acquired TTP with this ELISA. We observed a good correlation between the activities of anti-ADAMTS13 inhibitors determined by this ELISA and those given by the VWF multimer assay (Fig. 5B). The detection limit of VWF multimer and ELISA methods were 0.5 and 0.1 BUs per mL, respectively. A significant positive correlation with a coefficient of 0.99 was observed for 38 independent samples.

Levels of plasma ADAMTS13 activity

For 20 patients with USS who consistently exhibited plasma levels of ADAMTS13 activity less than 3 percent of normal levels by a classic VWF multimer assay, the value determined with this novel ELISA was less than 0.5 percent of normal levels in 16 patients. In the remaining 4 patients, the values ranged from 0.6 to 1.3 percent. USS carriers (n = 33) exhibited activities averaging 34.3 ± 12.3 percent (mean ± SD; Fig. 6). We have reported a very rare individual, the father of a patient with USS, who carries two ADAMTS13 gene mutations (R268P/P475S). He consistently exhibited very low levels of plasma ADAMTS13 activity (4.5-7%) by a classic VWF multimer assay.[21] He is now 38 years old, but so far he has no episode of thrombocytopenia or TTP. By our novel ELISA, this individual also showed low plasma ADAMTS13 activity (4.2%).

Of the 61 patients with acquired TTP, 29 patients had less than 3 percent of normal plasma ADAMTS13 activity, while 32 patients exhibited greater than 3 percent by classic VWF multimer assay. In these groups, the levels of plasma ADAMTS13 activity measured by the novel ELISA were 0.7 ± 0.5 and 13.8 ± 10.3 percent, respectively. In normal individuals, plasma level of ADAMTS13 activity measured under these conditions averaged 99.1 ± 21.5 percent (26 male, 97.1 ± 18.1%; 29 female, 100.1 ± 24.4%; Fig. 6).

The ADAMTS13 activities measured by either ELISA or the classic VWF multimer assay were compared for the three groups of USS patients and carriers, patients with acquired TTP, and normal individuals (Fig. 7). The regression line for the three groups were $y = 0.67x + 3.51$, $y = 1.15x + 1.40$, and $y = 0.90x + 10.05$, respectively. The correlation coefficients for the three groups were $r = 0.82$, $r = 0.79$, and $r = 0.85$, respectively.

DISCUSSION

We have developed a convenient and highly sensitive ELISA measuring ADAMTS13 activity. We prepared mouse MoAbs that recognized the C-terminal edge residue Y1605 of the VWF-A2 domain that is exposed by ADAMTS13 cleavage. Two synthetic peptides, N15 and N10, derived from the VWF-A2 domain were prepared and used as immunogens. We have obtained a number of MoAb clones specific for both peptides and used one MoAb from each group for further studies. Anti-N15 MoAb reacted with both the N15 peptide and GST-VWF73-His, but did not react with N10, GST-VWF10, or the 250-kDa VWF subunit, indicating that the epitope includes the 1605-YM-1606 bond within the VWF-A2 domain, which is cryptic in the full-length VWF subunit. In contrast, the anti-N10 MoAb reacted with the N10 peptide, GST-VWF10, the dimer of the N-terminal VWF subunit, and the monomer of the N-terminal 140-kDa band, but did not react with other synthetic peptides, GST-VWF73-His, or the undigested 250-kDa VWF subunit. Studies with a panel of N10-related

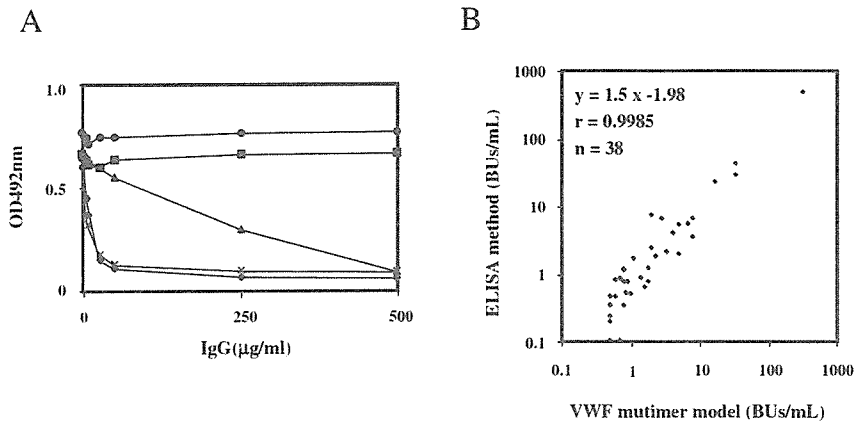

Fig. 5. Effect of antibodies in this ELISA and levels of plasma anti-ADAMTS13 inhibitor. Pooled undiluted normal plasma was incubated for 2 hours at 37°C with varying concentrations of purified IgGs. The residual activity of ADAMTS13 in this mixture was then determined. (A) Purified IgG from normal subjects (■) and normal mouse IgG (●) did not exhibit any significant inhibition at any of the concentrations tested; samples from patients with acquired TTP (▲) demonstrated a dose-dependent inhibition. Of two anti-ADAMTS13 MoAbs generated in this study, both the A10 antibody (×) and the anti-N15 MoAb (No. 73; ◆) completely inhibited ADAMTS13 activity at a concentration of 20 μg/mL. (B) The measurements of anti-ADAMTS13 inhibitor concentration by this ELISA and the VWF multimer assay correlated well. The inhibitor detection limit for the VWF multimer and ELISA methods were 0.5 and 0.1 BUs per mL, respectively. A significant positive correlation with a coefficient of 0.99 was observed for 38 independent samples.

synthetic peptides indicated that the crucial epitope for anti-N10 MoAb requires Y1605 to be the C-terminal residue, but also recognizes a conformation created by the nanopeptide sequence (1597-REQAPNLVY-1605). This recognition pattern allows the use of this MoAb in our novel ELISA, as the C-terminal Y1605 residue is exposed by the cleavage of full-length VWF by ADAMTS13.

When we performed an ELISA with GST-VWF73-His as a substrate and HRP-labeled anti-N10 MoAb as a second antibody, reactivity increased in proportion to the amount of enzyme added. Next we optimized reaction conditions of this ELISA, because ADAMTS13 requires the presence of divalent cations for its activity. In our novel ELISA, Mg^{2+} was most efficient for expressing the proteolytic activity. This result appeared to be slightly different from previous studies, because Ba^{2+} was optimal in the VWF multimer assay with native VWF as substrate,[30] whereas Ca^{2+} was most efficient in FRETS-VWF73 assay. This inconsistency is apparently caused by the difference of substrate species and reaction conditions, including protein denaturants and pH. Thus, we have included 5 mmol per L $MgCl_2$ in the reaction mixture of our assay. We confirmed the specificity of this novel ELISA by inhibition with EDTA and with a variety of well-characterized MoAbs. As a result, this novel ELISA is superior to previously reported assays.

The first advantage of this assay is the increased sensitivity. The lower limit of this assay was determined to be 0.5 percent of the normal control, in contrast to that of conventional assays at 3 to 5 percent. The sensitivity of this assay provided us with new information about USS and acquired TTP. For example, the novel ELISA demonstrated that 16 of 20 USS patients had plasma levels of ADAMTS13 activity below 0.5 percent of the normal control. The remaining 4 patients, however, had the values of 0.6 to 1.3 percent. Interestingly, an asymptomatic carrier with R268P/P475S gene mutations, the father of a USS patient, showed 4.2 percent of the activity by this ELISA. This may indicate that the plasma level of ADAMTS13 activity between 1.3 and 4.2 percent is a range essentially important to regulate the manifestation of clinical signs of TTP, unless other precipitating factors are present. Prophylactic infusions with a small amount of fresh-frozen plasma (approx. 5 mL/kg, every 2-3 weeks) to USS patients, which is effective at preventing the clinical manifestations, may support our speculation. Further, in patients with acquired TTP with less than 3 percent of ADAMTS13 activity by a VWF multimer assay, this ELISA showed that 23 of 29 had ADAMTS13 activity below 0.5 percent, and the remaining six patients had the values of 0.6 to 2.6 percent.

The second advantage of this assay is the sensitivity of measurement for inhibitors of ADAMTS13. The existence of inhibitors of ADAMTS13 is the key to diagnosing acquired TTP. The levels of plasma inhibitors against ADAMTS13 are also an indicator of the efficacy of therapy, typically plasma exchange or corticosteroids, in patients with acquired TTP. It is difficult, however, to determine accurately the low titers of plasma inhibitors of ADAMTS13 with conventional methods. The detection limit for inhibitors in this novel ELISA was calculated at 0.1 BU per mL. Inhibitor levels under 0.5 BU per mL, the lower limit of a VWF multimer assay, were detected in five patients with acquired TTP with this ELISA. Further investigation will be required to identify the significance of low titer inhibitors.

The third advantage of this ELISA is convenience of its performance in hospital environments, because it does not require any special technique or instrument except for standard ELISA equipment routinely used in many laboratories. As a consequence, we have established a convenient and highly sensitive MoAb-based ELISA to measure

ADAMTS13 activity. The values determined by this method correlated well with those determined by classic VWF multimer assay. Because this novel assay utilizes MoAbs, it may be possible to develop a rapid, automated assay to assess ADAMTS13 activity based on this technology.

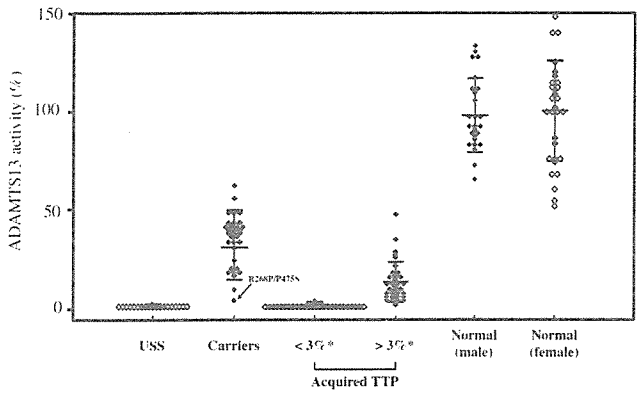

Fig. 6. Plasma levels of ADAMTS13 activity in normal subjects and patients with TTP. Plasma levels of ADAMTS13 activity in 16 patients with USS, determined by the novel ELISA, were less than 0.5 percent of normal levels; in the remaining four patients, activities ranged from 0.6 to 1.3 percent of normal. USS carriers (n = 33) exhibited an average activity of 34.3 ± 12.3 percent (mean ± SD). Of 61 patients with acquired TTP, 29 patients had less than 3 percent and 32 patients displayed greater than 3 percent of normal plasma ADAMTS13 activity by the VWF multimer method. In these two groups, the levels of plasma ADAMTS13 activity by the novel ELISA were 0.7 ± 0.5 and 13.8 ± 10.3 percent, respectively. In normal individuals, our novel ELISA gave a mean plasma ADAMTS13 activity of 99.1 ± 21.5 percent (26 male, 97.9 ± 18.1%; 29 female, 100.1 ± 24.4%).

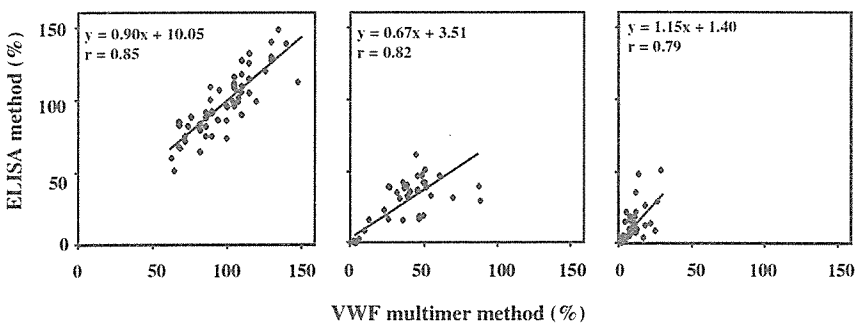

Fig. 7. Correlation of ADAMTS13 activity between ELISA and VWF multimer method. ADAMTS13 activities, measured by ELISA or the VWF multimer method, were compared for samples divided into three groups of patients with USS and carriers (middle, n = 53), patients with acquired TTP (right, n = 61), and normal individuals (left, n = 55). Significant positive correlations were observed in all three groups.

REFERENCES

1. Moschcowitz E. Hyalin thrombosis of the terminal arterioles and capillaries: a hitherto undescribed disease. Proc N Y Pathol Soc 1924;24:21-4.
2. Zheng XL, Kaufman RM, Goodnough LT, Sadler JE. Effect of plasma exchange on plasma ADAMTS13 metalloprotease activity, inhibitor level, and clinical outcome in patients with idiopathic and nonidiopathic thrombotic thrombocytopenic purpura. Blood 2004;103:4043-9.
3. Vesely SK, George JN, Lämmle B, et al. ADAMTS13 activity in thrombotic thrombocytopenic purpura–hemolytic uremic syndrome: relation to presenting features and clinical outcomes in a prospective cohort of 142 patients. Blood 2003;102:60-8.
4. Gerritsen HE, Robles R, Lämmle B, Furlan M. Partial amino acid sequence of purified von Willebrand factor-cleaving protease. Blood 2001;98:1654-61.
5. Fujikawa K, Suzuki H, McMullen B, Chung D. Purification of human von Willebrand factor-cleaving protease and its identification as a new member of the metalloproteinase family. Blood 2001;98:1662-6.
6. Zheng X, Chung D, Takayama TK, et al. Structure of von Willebrand factor cleaving protease (ADAMTS13), a metalloprotease involved in thrombotic thrombocytopenic purpura. J Biol Chem 2001;276:41059-63.
7. Soejima K, Mimura N, Hirashima M, et al. A novel human metalloprotease synthesized in the liver and secreted into the blood: possibly, the von Willebrand factor-cleaving protease? J Biochem 2001;130:475-80.
8. Levy GG, Nichols WC, Lian EC, et al. Mutations in a member of the ADAMTS gene family cause thrombotic thrombocytopenic purpura. Nature 2001;413:488-94.
9. Plaimauer B, Zimmerman K, Volke ID, et al. Cloning expression and characterization of the von Willebrand factor-cleaving protease (ADAMTS13). Blood 2002;100:3626-32.
10. Furlan M, Robles R, Galbusera M, et al. von Willebrand factor-cleaving protease in thrombotic thrombocytopenic purpura and the hemolytic–uremic syndrome. N Engl J Med 1998;339:578-1584.
11. Tsai HM, Lian EC. Antibodies to von Willebrand factor-cleaving protease in acute thrombotic thrombocytopenic purpura. N Engl J Med 1998;339:1585-94.
12. Fujimura Y, Matsumoto M, Yagi H, et al. von Willebrand factor-cleaving protease and Upshaw–Schulman syndrome. In: Progress in Hematology. Int J Hematol 2002;75:25-34.
13. Uemura M, Tatsumi K, Matsumoto M, et al. Localization of ADAMTS13 to the stellate cells of human liver. Blood 2005;106:922-4.

14. Yagi H, Konno M, Kinoshita S, et al. Plasma of patients with Upshaw–Schulman syndrome, a congenital deficiency of von Willebrand factor-cleaving protease activity, enhances the aggregation of normal platelets under high shear stress. Br J Haematol 2001;115:991-7.
15. Kokame K, Matsumoto M, Fujimura Y, Miyata T. VWF73, a region from D1596 to R1668 of von Willebrand factor, provides a minimal substrate for ADAMTS-13. Blood 2004;103:607-12.
16. Zhou W, Tsai HM. An enzyme immunoassay of ADAMTS13 distinguishes patients with thrombotic thrombocytopenic purpura from normal individuals and carriers of ADAMTS13 mutations. Thromb Haemost 2004;91:806-11.
17. Whitelock JL, Nolasco L, Bernardo A, et al. ADAMTS-13 activity in plasma is rapidly measured by a new ELISA method that uses recombinant VWF-A2 domain as substrate. J Thromb Haemost 2004;2:485-91.
18. Kokame K, Nobe Y, Kokubo Y, Okayama A, Miyata T. FRETS-VWF73, a first fluorogenic substrate for ADAMTS13 assay. Br J Haematol 2005;129:93-100.
19. Kasper CK, Aledort LM, Counts RB, et al. A more uniform measurement of factor VIII inhibitors. Thromb Diath Haemorrh 1975;34:869-72.
20. Warkentin TE, Kelton JG. Acquired platelet disorders. In: Bloom AL, Forbes CD, Thomas DP, Tuddenham EG, editors. Hemostasis and thrombosis, Vol. 2. London: Churchill Livingstone; 1994. p. 767-815.
21. Kokame K, Matsumoto M, Soejima K, et al. Mutations and common polymorphisms in ADAMTS13 gene responsible for von Willebrand factor-cleaving protease activity. Proc Natl Acad Sci U S A 2002;99:11902-7.
22. Matsumoto M, Kokame K, Soejima K, et al. Molecular characterization of ADAMTS13 gene mutations in Japanese patients with Upshaw–Schulman syndrome. Blood 2004; 103:1305-10.
23. Uchida T, Wada H, Mizutani M, et al. Identification of novel mutations in ADAMTS13 in an adult patients with congenital thrombotic thrombocytopenic purpura. Blood 2004;104:2081-3.
24. Shibagaki Y, Matsumoto M, Kokame K, et al. Novel compound heterozygote mutations (H234Q/R1206X) of the ADAMTS13 gene in an adult patient with Upshaw–Schulman syndrome showing predominant episodes of repeated acute renal failure. Nephrol Dial Transpl 2006; 21:1289-92.
25. Köhler G, Milstein C. Continuous cultures of fused cells secreting antibody of predefined specificity. Nature 1975;256:495-7.
26. Hamaguchi Y, Yoshitake S, Ishikawa E, Endo Y, Ohtaki S. Improve procedure for the conjugation of rabbit IgG and Fab' antibodies with beta-D-galactosidase from Escherichia coli using N,N'-o-phenylendimaleimidase. J Biochem (Tokyo) 1979;85:1289-300.
27. Yoshitake S, Imagawa M, Ishikawa E, et al. Mild and efficient conjugation of rabbit Fab' and horseradish peroxidase using a maleimide compound and its use for enzyme immunoassay. J Biochem (Tokyo) 1982;92:1413-24.
28. Laemmli UK. Cleavage of structural proteins during the assembly of the head of bacteriophage T4. Nature 1970; 227:680-5.
29. Schägger H, von Jagow G. Tricine-sodium dodesyl sulfate-polyacrylamide gel electrophoresis for the separation of proteins in the range from 1 to 100 kDa. Anal Biochem 1987;166:368-79.
30. Furlan M, Robles R, Lämmle B. Partial purification and characterization of a protease from human plasma cleaving von Willebrand factor to fragments produced by in vivo proteolysis. Blood 1996;87:4223-34.

Adiponectin Acts as an Endogenous Antithrombotic Factor

Hisashi Kato, Hirokazu Kashiwagi, Masamichi Shiraga, Seiji Tadokoro, Tsuyoshi Kamae, Hidetoshi Ujiie, Shigenori Honda, Shigeki Miyata, Yoshinobu Ijiri, Junichiro Yamamoto, Norikazu Maeda, Tohru Funahashi, Yoshiyuki Kurata, Iichiro Shimomura, Yoshiaki Tomiyama, Yuzuru Kanakura

Objective—Obesity is a common risk factor in insulin resistance and cardiovascular diseases. Although hypoadiponectinemia is associated with obesity-related metabolic and vascular diseases, the role of adiponectin in thrombosis remains elusive.

Methods and Results—We investigated platelet thrombus formation in adiponectin knockout (APN-KO) male mice (8 to 12 weeks old) fed on a normal diet. There was no significant difference in platelet counts or coagulation parameters between wild-type (WT) and APN-KO mice. However, APN-KO mice showed an accelerated thrombus formation on carotid arterial injury with a He-Ne laser (total thrombus volume: $13.36\pm4.25\times10^7$ arbitrary units for APN-KO and $6.74\pm2.87\times10^7$ arbitrary units for WT; n=10; $P<0.01$). Adenovirus-mediated supplementation of adiponectin attenuated the enhanced thrombus formation. In vitro thrombus formation on a type I collagen at a shear rate of 250 s^{-1}, as well as platelet aggregation induced by low concentrations of agonists, was enhanced in APN-KO mice, and recombinant adiponectin inhibited the enhanced platelet aggregation. In WT mice, adenovirus-mediated overexpression of adiponectin additionally attenuated thrombus formation.

Conclusion—Adiponectin deficiency leads to enhanced thrombus formation and platelet aggregation. The present study reveals a new role of adiponectin as an endogenous antithrombotic factor. (***Arterioscler Thromb Vasc Biol.* 2006;26:224-230.**)

Key Words: acute coronary syndromes ■ obesity ■ platelets ■ thrombosis

Obesity is associated with insulin resistance, accelerated atherothrombosis, and cardiovascular diseases.[1,2] Recent studies have revealed that adipose tissue is not only a passive reservoir for energy storage but also produces and secretes a variety of bioactive molecules, known as adipocytokines, including tumor necrosis factor (TNF) α, leptin, resistin, and plasminogen activator inhibitor type-1.[2–4] Dysregulated production of adipocytokines participates in the development of obesity-related metabolic and vascular diseases.[2–4]

Adiponectin is an adipocytokine identified in the human adipose tissue cDNA library, and Acrp30/AdipoQ is the mouse counterpart of adiponectin (reviewed in reference[5]). Adiponectin, of which mRNA is exclusively expressed in adipose tissue, is a protein of 244 amino acids consisting of 2 structurally distinct domains, an N-terminal collagen-like domain and a C-terminal complement C1q-like globular domain. Adiponectin is abundantly present in plasma (5 to 30 μg/mL), and its plasma concentration is inversely related to the body mass index.[5] Plasma adiponectin levels decrease in obesity, type 2 diabetes, and patients with coronary artery disease (CAD).[5–9] Indeed, adiponectin (APN) knockout (KO) mice showed severe diet–induced insulin resistance.[10] In cultured cells, we have demonstrated that human recombinant adiponectin inhibited the expression of adhesion molecules on endothelial cells, the transformation of macrophages to foam cells, and TNF-α production from macrophages.[5,11] Furthermore, APN-KO mice showed severe neointimal thickening in mechanically injured arteries.[12] Adenovirus-mediated supplementation of adiponectin attenuated the development of atherosclerosis in apolipoprotein E–deficient mice as well as postinjury neointimal thickening in APN-KO mice.[12,13] These data suggest the antiatherogenic properties of adiponectin, and, hence, hypoadiponectinemia may be associated with a higher incidence of vascular diseases in obese subjects. Although it is also possible that an altered hemostatic balance may contribute to the pathogenesis of acute cardiovascular events in such patients, the roles of adiponectin in hemostasis and thrombosis remains elusive.

Original received August 4, 2005; final version accepted October 24, 2005.

From the Departments of Hematology and Oncology (H. Kato, H. Kashiwagi, M.S., S.T., T.K., H.U., Y.T., Y.Ka.) and Internal Medicine and Molecular Science (N.M., T.F., I.S.), Graduate School of Medicine, Osaka University, Suita; National Cardiovascular Center Research Institute (S.H.), Suita, Osaka; Division of Transfusion Medicine (S.M.), National Cardiovascular Center, Suita, Osaka; Department of Nutrition Management (Y.I.), Faculty of Health Science, Hyogo University, Kakogawa, Hyogo; Laboratory of Physiology, Faculty of Nutrition (J.Y.) and High Technology Research Centre (J.Y.), Kobe Gakuin University, Kobe; and Department of Blood Transfusion (Y.Ku.), Osaka University Hospital, Suita, Japan.

Correspondence to Yoshiaki Tomiyama, Osaka University, Department of Hematology and Oncology, 2-2 Yamadaoka, Suita, Osaka 565-0871, Japan. E-mail yoshi@hp-blood.med.osaka-u.ac.jp

Arterioscler Thromb Vasc Biol. is available at http://www.atvbaha.org

DOI: 10.1161/01.ATV.0000194076.84568.81

Here we have provided the first evidence that adiponectin affects thrombus formation, and, hence, hypoadiponectinemia may directly contribute to acute coronary syndrome. Our data indicate a new role of adiponectin as an antithrombotic factor.

Methods

Mice

APN-KO male mice (8 to 12 weeks old) were generated as described previously.[10,12] We analyzed mice backcrossed to C57BL/6 for 5 generations.[10,12]

Preparation of Mouse Platelets and Measurement of Coagulation Parameters

Mouse platelet-rich plasma (PRP) was obtained as described previously.[14] Coagulation parameters were measured by SRL Inc.

Platelet Aggregation Study, Adhesion Study, and Flow Cytometry

Platelet aggregation and platelet adhesion study was performed as described previously.[14] Integrin $\alpha_{IIb}\beta_3$ activation and α-granule secretion of wild-type (WT) and APN-KO platelets were detected by phycoerythrin-conjugated JON/A monoclonal antibody (mAb), which binds specifically to mouse-activated $\alpha_{IIb}\beta_3$ (Emfret Analytics) and FITC-conjugated anti-P-selectin mAb (Becton Dickinson), respectively.[14]

Assessment of Atherosclerosis and Bleeding Time Measurement

Assessment of atherosclerosis was performed as described previously.[15] The tail of anesthetized mice (nembutal 65 mg/kg; 8 to 12 weeks old) was transected 5 mm from the tip and then immersed in 0.9% isotonic saline at 37°C. The point until complete cessation of bleeding was defined as the bleeding time.

He-Ne Laser–Induced Thrombosis

The observation of real-time thrombus formation in the mouse carotid artery was performed as described previously.[15] Anesthetized mice (nembutal 65 mg/kg) were placed onto a microscope stage, and the left carotid artery (450 to 500 μm in diameter) was gently exposed. Evans blue dye (20 mg/kg) was injected into the left femoral artery via an indwelt tube, and then the center of the exposed carotid artery was irradiated with a laser beam (200 μm in diameter at the focal plane) from a He-Ne laser (Model NEO-50MS; Nihon Kagaku Engineering Co, Ltd). Thrombus formation was recorded on a videotape through a microscope with an attached CCD camera for 10 minutes. The images were transferred to a computer every 4 s, and the thrombus size was analyzed using Image-J software (National Institutes of Health). We calculated thrombus size by multiplying each area value and its grayscale value together. We then regarded the total size values for an individual thrombus obtained every 4 s during a 10-minute observation period as the total thrombus volume and expressed them in arbitrary units.

Flow Chamber and Perfusion Studies

The real-time observation of mural thrombogenesis on a type I collagen-coated surface under a shear rate of 250 s^{-1} was performed as described previously.[16] Briefly, whole blood obtained from anesthetized mice was anticoagulated with argatroban, and then platelets in the whole blood were labeled by mepacrine. Type I collagen-coated glass cover slips were placed in a parallel plate flow chamber (rectangular type; flow path of 1.9-mm width, 31-mm length, and 0.1-mm height). The chamber was assembled and mounted on an epifluorescence microscope (Axiovert S100 inverted microscope, Carl Zeiss Inc) with the computer-controlled z-motor (Ludl Electronic Products Lts). Whole blood was aspirated through the chamber, and the entire platelet thrombus formation process was observed in real time and recorded with a video recorder.

Preparation of Adenovirus and Recombinant Adiponectin

Adenovirus producing the full-length mouse adiponectin was prepared as described previously.[10] Plaque-forming units (1×10^8) of adenovirus-adiponectin (Ad-APN) or adenovirus-β-galactosidase (Ad-βgal) were injected into the tail vein. Experiments were performed on the fifth day after viral injection. The plasma concentrations of adiponectin were measured by a sandwich ELISA. Mouse and human recombinant proteins of adiponectin were prepared as described previously.[11,17]

RT-PCR

Total cellular RNA of platelets from WT or APN-KO mice was obtained, and contaminated genomic DNA was removed using a QuantiTect Reverse-Transcription kit (QIAGEN). One microgram of total RNA was used as a template for RT-PCR as described previously.[18] For the amplification of transcripts of mouse adiponectin receptors AdipoR1 and AdipoR2, the following primers were used: mouse AdipoR1 5′-ACGTTGGAGAGTCATCCCGTAT-3′ (sense) and 5′-CTCTGTGTGGATGCGGAAGAT-3′ (antisense) and mouse AdipoR2 5′-TGCGCACACATTTCAGTCTCCT-3′ (sense) and 5′-TTCTATGATCCCCAAAAGTGTGC-3′ (antisense).[19,20] For human platelet isolation, PRP obtained from 50 mL of whole blood was passed through a leukocyte removal filter as described previously.[21] This procedure removed >99.9% of the contaminated leukocytes.[21] For human AdipoR1 and AdipoR2, the following primers were used: human AdipoR1 5′-CTTCTACTGCTCCCCACAGC-3′ (sense) and 5′-GACAAAGCCCTCAGCGATAG-3′ (antisense) human AdipoR2 5′-GGACCGAGCAAAAGACTCAG-3′ (sense) and 5′-CACCCAGAGGCTGCTACTTC-3′ (antisense). In addition, total cellular RNA obtained from a megakaryocytic cell line, CMK, and that from a human monocytic cell line, THP-1 (positive control)[22] was examined in parallel. RT-PCR samples omitting reverse transcriptase were used as negative controls.

Statistical Analysis

Results were expressed as mean±SD. Differences between groups were examined for statistical significance using Student t test.

Results

Characteristics of Adiponectin-Deficient Mice and Assessment of Atherosclerotic Lesions

The basal profiles of APN-KO male mice have been previously described.[10,12] To exclude the effects of diet on APN-KO mice, we used APN-KO male mice (8 to 12 weeks old) fed on a normal diet in this study. There were no differences in platelet counts, PT, APTT, and plasma fibrinogen concentrations (Table I, available online at http://atvb.ahajournals.org). Histological analyses revealed that neither Oil Red O staining of the inner surface of whole aorta nor elastin-van Gieson staining of transverse sections of carotid arteries showed any apparent atherosclerotic lesions in WT or APN-KO mice (data not shown).

Bleeding Time in APN-KO Mice

To examine the effects of adiponectin deficiency on thrombosis and hemostasis, we studied bleeding time in APN-KO mice. The bleeding time in APN-KO mice was slightly but significantly shorter (96.9±34.9 s; n=30; $P<0.05$) than that in WT mice (130.9±52.1 s; n=30).

Enhanced Thrombus Formation in APN-KO Mice and Adiponectin Adenovirus Ameliorates the Thrombogenic Tendency

We next examined the effect of adiponectin deficiency on thrombus formation using the He-Ne laser-induced carotid

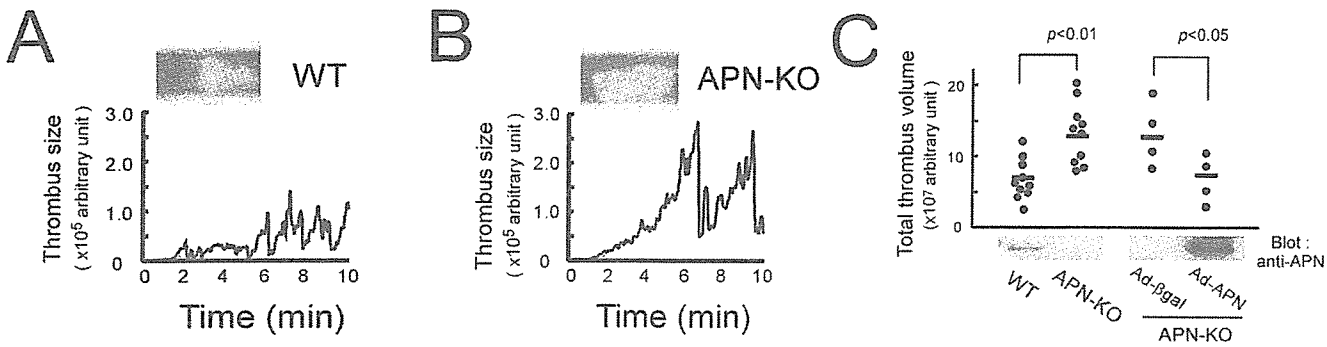

Figure 1. He-Ne laser–induced thrombus formation and adenovirus-mediated supplementation of adiponectin. Anesthetized mice were injected with Evans blue dye followed by irradiation with the He-Ne laser at the exposed left carotid artery. The representative time course of thrombus formation in (A) WT or (B) APN-KO mice is shown. (C) The total thrombus volume was significantly larger in APN-KO mice (n=10; $P<0.01$). In another set of experiments, administration of adenovirus-producing mouse adiponectin (Ad-APN) significantly attenuated the total thrombus volume, as compared with control adenovirus (Ad-βgal)-infected APN-KO mice (n=4; $P<0.05$). Plasma adiponectin levels detected in immunoblots are shown in the lower panel.

artery thrombus model. Endothelial injury of the carotid artery was induced by the interaction of Evans blue dye with irradiation from the He-Ne laser. In WT mice, thrombus formation started 61.0±25.0 s after the initiation of He-Ne laser irradiation (n=10). When the thrombi reached a certain size, they frequently ruptured and detached themselves from the wall because of increased shear stress. Thus, thrombus formation in this in vivo model showed a cyclic fluctuation, and complete occlusion was not observed (Figure 1). During a 10-minute observation period, the cycles of thrombus formation were 8.5±2.3 in WT mice. In APN-KO mice, there was no significant difference in the initiation time for thrombus formation (54.8±8.9 s; n=10; $P=0.46$). However, the cycles of thrombus formation during the 10-minute observation period were significantly fewer (5.4±2.0; n=10; $P<0.01$) in APN-KO mice. The thrombi in APN-KO mice grew larger and appeared to be stable and more resistant to the increased shear stress. Accordingly, the total thrombus volume was significantly larger in APN-KO mice ($6.74\pm2.87\times10^7$ arbitrary units in WT mice and $13.36\pm4.25\times10^7$ arbitrary units in APN-KO mice; n=10; $P<0.01$).

To confirm that adiponectin deficiency is responsible for the enhanced thrombus formation in APN-KO mice, we injected Ad-βgal or Ad-APN into APN-KO mice. On the fifth day after adenoviral injection, we confirmed the elevated plasma adiponectin level in Ad-APN-infected APN-KO mice in an ELISA assay (48.7±6.8 μg/mL; n=4), as well as in an immunoblot assay. In the carotid artery thrombus model, the total thrombus volume in Ad-βgal-infected APN-KO was $12.94\pm4.67\times10^7$ arbitrary units, which was compatible with that of APN-KO mice shown in Figure 1. In contrast, Ad-APN infection significantly decreased the total thrombus volume in APN-KO mice ($6.23\pm3.09\times10^7$ arbitrary units; n=4; $P<0.05$). These results indicate that adiponectin deficiency is responsible for the thrombogenic tendency in vivo.

Platelet-Thrombus Formation on Immobilized Collagen Under Flow Conditions

Because endothelial function may affect in vivo thrombus formation, we next performed in vitro mural thrombus formation on a type I collagen-coated surface under flow conditions. Figure 2 shows thrombus formation during a

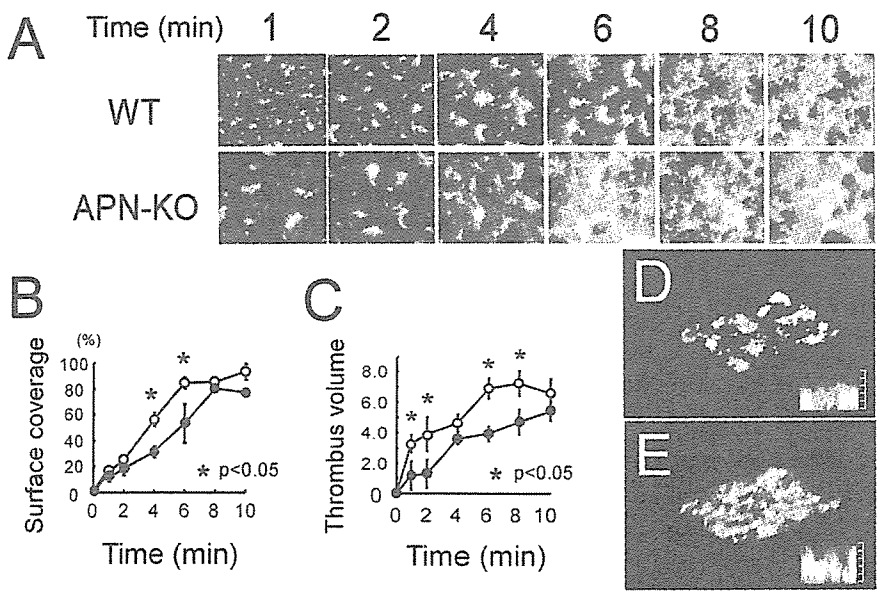

Figure 2. Thrombogenesis on a type I collagen-coated surface under flow conditions. (A) Mepacrine-labeled whole blood obtained from WT (top) or APN-KO mice (bottom) was perfused on a type I collagen-coated surface at a shear rate of 250 s^{-1}. (B) Platelet surface coverage (%) and (C) thrombus volume are shown at indicated time points. (●, WT; ○, APN-KO; *$P<0.05$). Shown are representative 3D images of thrombus formation at 6-minute perfusion in whole blood obtained from (D) WT and (E) APN-KO mice. Each inserted figure shows thrombus height.

10-minute perfusion of mouse whole blood anticoagulated with thrombin inhibitor at a low shear rate (250 s^{-1}). In whole blood obtained from WT mice, the thrombus fully covered the collagen-coated surface after 8 to 10 minutes of perfusion. In contrast, the thrombus grew more rapidly and fully covered the surface at 6 minutes in APN-KO mice. At 1 and 2 minutes of perfusion, there was no apparent difference in the initial platelet adhesion to the collagen surface between WT and APN-KO mice, whereas the platelet aggregate formation was significantly enhanced in APN-KO, even at 1 minute. We additionally examined the possibility that adiponectin might inhibit platelet adhesion onto collagen, because adiponectin binds to collagen types I, III, and V.[23] However, mouse recombinant adiponectin (40 μg/mL) did not inhibit the adhesion of platelets onto collagen, indicating that the inhibitory effect of adiponectin is not mediated by the inhibition of platelet binding to collagen (data not shown). At a high shear rate (1000 s^{-1}), the thrombus grew rapidly and fully covered the surface within 3 to 4 minutes. Under such strong stimuli, we did not detect any difference in thrombus formation between WT and APN-KO mice, probably because of the full activation of platelets.

Adiponectin Inhibits the Enhanced Platelet Aggregation in APN-KO Mice

In platelet aggregation studies, PRP obtained from APN-KO mice showed significantly enhanced platelet aggregation in response to low doses of agonists (ADP 2.5 μmol/L, collagen 2.5 μg/mL, and protease-activated receptor 4–activating peptide [PAR4-TRAP] 75 μmol/L), as compared with WT mice (Figure 3). The maximal platelet aggregation was achieved at higher concentrations of agonists, and the enhanced platelet aggregation in APN-KO mice was not apparent at these high doses of agonists, probably because of the full activation of platelets.

To confirm the inhibitory effect of adiponectin on platelet aggregation in vitro, we mixed 1 volume of PRP obtained from APN-KO mice with 4 volumes of platelet-poor plasma (PPP) obtained from APN-KO mice injected with either Ad-βgal or Ad-APN to adjust platelet counts to $300\times10^3/\mu L$. As shown in Figure 4A, the in vitro supplementation of PPP containing adiponectin attenuated the enhanced platelet aggregation. Similarly, in vitro administration of mouse recombinant adiponectin (40 μg/mL) to PRP from APN-KO mice attenuated the enhanced platelet aggregation (Figure 4B).

Expression of Adiponectin Receptors in Platelets and Effects of Adiponectin Deficiency on $\alpha_{IIb}\beta_3$ Activation and P-Selectin Expression

To reveal the effect of adiponectin on platelets, we examined whether platelets possess transcripts for adiponectin receptors AdipoR1 and AdipoR2 by using RT-PCR. As shown in Figure 5A, platelets from APN-KO, as well as WT mice, contained mRNAs for AdipoR1 and AdipoR2. We also confirmed that the human megakaryocytic cell line CMK, as well as carefully isolated human platelets, possessed mRNAs for AdipoR1 and AdipoR[2]. We next examined the effects of adiponectin deficiency on $\alpha_{IIb}\beta_3$ activation and α-granule secretion at various concentrations of agonists by flow cytometry. However, neither the platelet $\alpha_{IIb}\beta_3$ activation induced by ADP nor P-selectin expression induced by PAR4-TRAP showed significant difference between WT and APN-KO mice (n=4; Figure 5B and 5C).

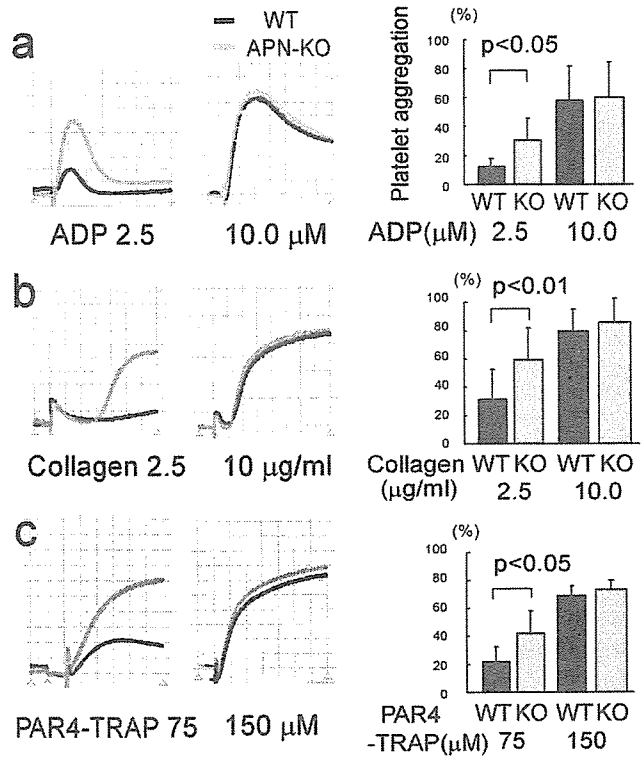

Figure 3. Enhanced platelet aggregation in APN-KO mice. Platelet aggregation in PRP obtained from WT or APN-KO mice. PRP ($300\times10^3/\mu L$) obtained from WT (black line) or APN-KO mice (gray line) was stimulated with ADP (a; n=4), collagen (b; n=4), or PAR4-TRAP (c; n=3). As compared with WT mice, platelet aggregation was enhanced in APN-KO mice at low concentrations of agonists.

Adiponectin Adenovirus Attenuates Thrombus Formation in WT Mice

Because WT mice have large amounts of adiponectin in their plasma, we, therefore, examined whether adiponectin overexpression could additionally inhibit thrombus formation, as well as platelet function, in WT mice. After the administration of Ad-APN or Ad-βgal into WT mice, the plasma adiponectin levels in Ad-APN-infected mice reached ≈4 times higher than those in Ad-βgal-infected WT mice (8.5±0.6 μg/mL for Ad-βgal and 37.0±14.8 μg/mL for Ad-APN; n=5). As shown in Figure 6A, platelet aggregation in PRP induced by collagen or PAR4-TRAP was significantly attenuated by the overexpression of adiponectin. Similarly, in vitro administration of human recombinant adiponectin (40 μg/mL) to human PRP attenuated the platelet aggregation response to 2.5 μg/mL collagen (Figure 6B). Moreover, in the He-Ne laser–induced carotid artery thrombus model, the overexpression of adiponectin significantly inhibited thrombus formation in WT mice ($4.38\pm0.75\times10^7$ arbitrary units for Ad-βgal and $2.75\pm0.61\times10^7$ arbitrary units for Ad-APN; n=7; $P<0.05$; Figure 6C).

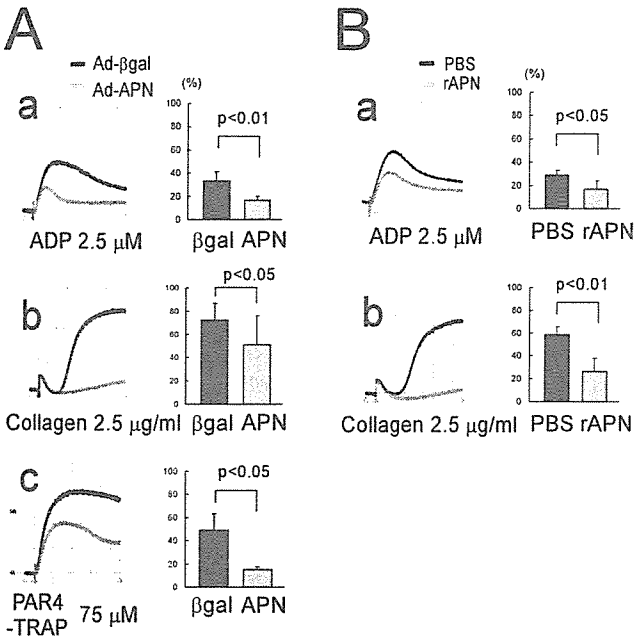

Figure 4. Effects of in vitro supplementation of adiponectin or recombinant adiponectin on the enhanced platelet aggregation in APN-KO mice. (A) One volume of PRP from APN-KO mice was mixed with ≈4 volumes of PPP from APN-KO mice injected with Ad-βgal (black line) or Ad-APN (gray line) to obtain a platelet concentration of $300\times10^3/\mu L$. Platelets were stimulated with indicated agonists (n=4). (B) Mouse recombinant adiponectin (40 μg/mL, gray line) or PBS (black line) was added to PRP from APN-KO mice. Platelets were adjusted to 300×10^3 platelets/μL and stimulated with indicated agonists (n=4).

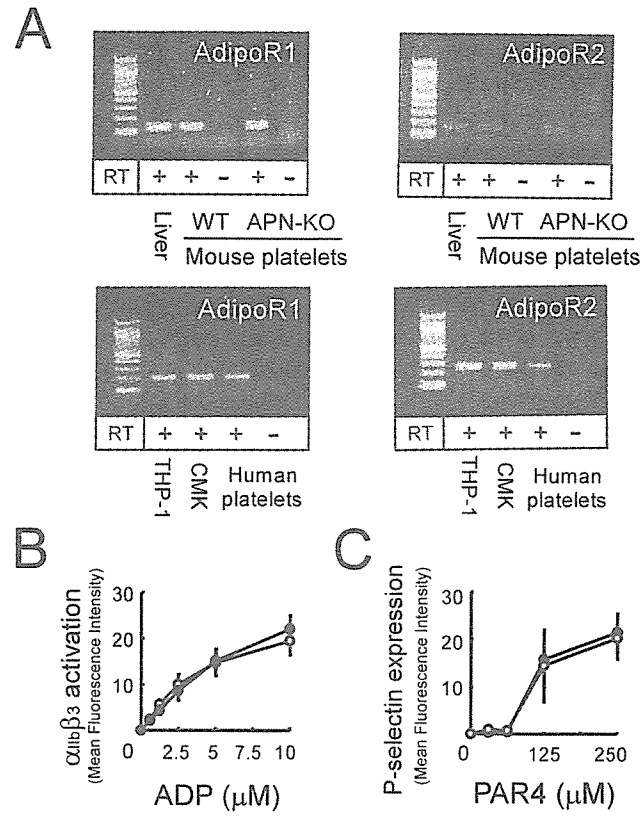

Figure 5. Expression of adiponectin receptors and effects of adiponectin deficiency on platelet function. (A, top) Expressions of transcripts for adiponectin receptors, AdipoR1 (133-bp fragments) and AdipoR2 (156-bp fragments), in platelets from WT or APN-KO mice were examined by RT-PCR. The liver was used as a positive control. (Bottom) Expressions of transcripts for adiponectin receptors, AdipoR1 (196-bp fragments) and AdipoR2 (243-bp fragments), in CMK cells, as well as human platelets, were examined by RT-PCR; 100-bp DNA Ladder (New England Biolabs) was used as a marker. Effects of adiponectin deficiency on (B) $\alpha_{IIb}\beta_3$ activation and (C) α-granule secretion. PRP obtained from WT (●) or APN-KO (○) mice in the presence of phycoerythrin-JON/A mAb or FITC-anti-P-selectin mAb was stimulated with the indicated agonist and then analyzed by flow cytometry without any washing. There were no significant differences in platelet $\alpha_{IIb}\beta_3$ activation or P-selectin expression between WT and APN-KO mice (n=4).

Discussion

In the present study, we have newly revealed an antithrombotic effect of adiponectin. APN-KO male mice (8 to 12 weeks old) fed on a normal diet showed no significant differences in platelet counts and coagulation parameters compared with WT mice. In the He-Ne laser–induced carotid artery thrombus model, APN-KO mice showed an accelerated thrombus formation, and adenovirus-mediated supplementation of adiponectin attenuated this enhanced thrombus formation. Platelet aggregometry and the real-time observation of in vitro thrombus formation on a type I collagen-coated surface under flow conditions showed the enhanced platelet function in APN-KO mice. Moreover, adenovirus-mediated overexpression of adiponectin attenuated in vivo thrombus formation, as well as the in vitro platelet aggregation response, even in WT mice. Thus, the present data strongly suggest that adiponectin possesses an antithrombotic potency.

We have demonstrated that low concentrations of adiponectin are associated with the prevalence of CAD in men, which is independent of well-known CAD risk factors.[8] Pischon et al[9] have recently shown that high concentrations of adiponectin are associated with a lower risk of myocardial infarction in men, which is also independent of inflammation and glycemic status and can be only partly explained by differences in blood lipids. These clinical studies suggest that the protective effect of adiponectin on the development of CAD may be primary rather than secondary through the protection of metabolic abnormalities, such as insulin resistance. Indeed, APN-KO mice fed on a normal diet did not show any abnormalities in plasma glucose, insulin, or lipid profiles.[10,12] Although the atherosclerotic and thrombotic processes are distinct from each other, these processes appear to be interdependent, as shown by the term *atherothrombosis*. The interaction between the vulnerable atherosclerotic plaque, which is prone to disruption, and thrombus formation is the cornerstone of acute coronary syndrome (ACS).[24] In this context, our present data strongly suggest that adiponectin deficiency (or hypoadiponectinemia) may directly contribute to the development of ACS by enhanced platelet thrombus formation.

Although APN-KO fed on a normal diet showed no significant differences in major metabolic parameters, they showed delayed clearance of FFA in plasma, elevated plasma TNF-α concentrations (≈40 pg/mL in APN-KO; ≈20 pg/mL in WT), and elevated CRP mRNA levels in white adipose tissue.[12,25] In addition, recombinant adiponectin increased NO production in vascular endothelial cells.[26] To rule out any

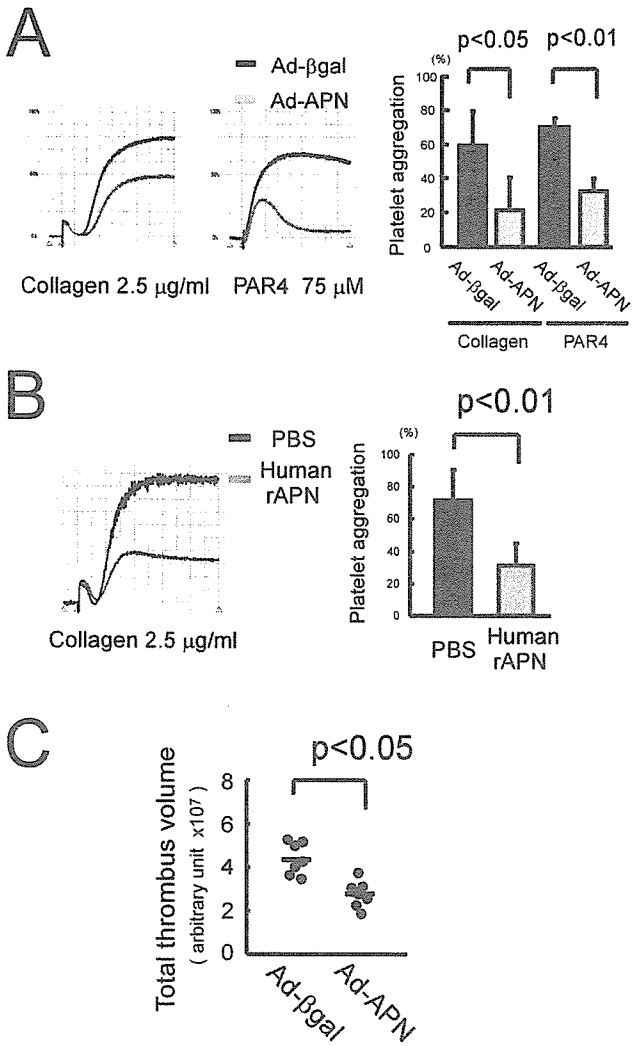

Figure 6. Overexpression of adiponectin additionally attenuates thrombus formation in WT mice. (A) Platelet aggregation in PRP obtained from WT mice injected with either Ad-βgal or Ad-APN. PRP ($300\times10^3/\mu L$) obtained from WT mice injected with either Ad-βgal (black line) or Ad-APN (gray line) was stimulated with collagen or PAR4-TRAP (n=4). Administration of Ad-APN significantly attenuated platelet aggregation in WT mice. (B) Human recombinant adiponectin (40 μg/mL, gray line) or PBS (black line) was added to PRP ($300\times10^3/\mu L$) from control subjects. Platelets were stimulated with collagen (n=7). (C) He-Ne laser–induced thrombus formation in WT mice injected with either Ad-βgal or Ad-APN. Administration of Ad-APN in WT mice additionally reduced the total thrombus volume in the carotid artery thrombus model (n=7, $P<0.05$).

effect of adiponectin on vascular cells, we examined in vitro thrombus formation on a type I collagen-coated surface under flow conditions, as well as platelet aggregation in APN-KO mice. Thus, the enhanced platelet function in APN-KO mice was still evident even in the absence of vascular cells. Moreover, human and mouse recombinant adiponectin attenuated the aggregation response obtained from control human subjects and from APN-KO mice, respectively. Thus, adiponectin inhibits platelet function. However, the mechanism by which adiponectin attenuates platelet aggregation and arterial thrombus formation in vivo remains unclear. During thrombogenesis, platelets adhere to altered vascular surfaces or exposed subendothelial matrices, such as collagen, and then become activated and aggregate to each other.[16] The thrombus formed in APN-KO mice appeared to be stable and more resistant to the increased shear stress, without affecting the initiation time for thrombus formation in carotid artery injury experiments, as well as in flow chamber perfusion experiments. In addition, preincubation of collagen with recombinant adiponectin did not inhibit platelet adhesion on collagen under static conditions. Thus, it is unlikely that the inhibitory effect of adiponectin is mediated by the inhibition of platelet binding to collagen. These characteristics are quite distinct from C1q-TNF–related protein-1, which belongs to the same family as adiponectin and inhibits thrombus formation by interfering with platelet–collagen interaction.[27] We confirmed that transcripts for AdipoR1 and AdipoR2 were present in mouse and human platelets and CMK cells. Although the platelet–platelet interaction appeared to be enhanced in APN-KO mice, we did not detect any difference in agonist-induced $\alpha_{IIb}\beta_3$ activation or P-selectin expression between APN-KO and WT mice by flow cytometry. Based on these results, it is possible that adiponectin may inhibit $\alpha_{IIb}\beta_3$-mediated intracellular postligand binding events. Alternatively, previous studies have shown that adiponectin is physically associated with many proteins, including α_2-macroglobulin, thrombospondin-1 (TSP-1), and several growth factors.[5,23,28] Interestingly, TSP-1, after secretion from platelet α granules, may participate in platelet aggregation by reinforcing interplatelet interactions through direct fibrinogen-TSP-fibrinogen and TSP-TSP crossbridges.[29,30] In this context, it is also possible that it may interfere with interplatelet interactions in platelet aggregation. Additional studies to clarify the mechanism of adiponectin are currently under way.

In conclusion, our present study revealed that adiponectin acts as an endogenous antithrombotic factor. Although it is possible that the in vivo antithrombotic effect of adiponectin may be partly mediated by its action on vascular cells, our present data clearly indicate that adiponectin affects platelet function in the absence of vascular cells. In addition, the overexpression of adiponectin in WT mice attenuates in vivo thrombus formation, as well as the in vitro platelet aggregation response. Our data provide a new insight into the pathophysiology of ACS in nonobese, as well as obese, subjects, and adiponectin (and its derivatives) may be a new candidate for an antithrombotic drug.

Acknowledgments

This study was supported in part by Grant-in-Aid for Scientific Research from the Ministry of Education, Culture, Sports, Science, and Technology in Japan; from the Ministry of Health, Labor, and Walfare in Japan, Astellas Foundation for Research on Metabolic Disorder, Tokyo, Japan; and Mitsubishi Pharma Research Foundation, Osaka, Japan.

References

1. Spiegelman BM, Flier JS. Obesity and the regulation of energy balance. *Cell.* 2001;104:531–543.
2. Friedman JM. Obesity in the new millennium. *Nature.* 2000;404:632–634.
3. Hotamisligil GS, Shargill NS, Spiegelman BM. Adipose expression of tumor necrosis factor-α: direct role in obesity-linked insulin resistance. *Science.* 1993;259:87–91.

4. Steppan CM, Bailey ST, Bhat S, Brown EJ, Banerjee RR, Wright CM, Patel HR, Ahima RS, Lazar MA. The hormone resistin links obesity to diabetes. *Nature.* 2001;409:307–312.
5. Matsuzawa Y, Funahashi T, Kihara S, Shimomura I. Adiponectin and metabolic syndrome. *Arterioscler Thromb Vasc Biol.* 2004;24:29–33.
6. Hotta K, Funahashi T, Arita Y, Takahashi M, Matsuda M, Okamoto Y, Iwahashi H, Kuriyama H, Ouchi N, Maeda K, Nishida M, Kihara S, Sakai N, Nakajima T, Hasegawa K, Muraguchi M, Ohmoto Y, Nakamura T, Yamashita S, Hanafusa T, Matsuzawa Y. Plasma concentrations of a novel, adipose-specific protein, adiponectin, in type 2 diabetic patients. *Arterioscler Thromb Vasc Biol.* 2000;20:1595–1599.
7. Zoccali C, Mallamaci F, Tripepi G. Novel cardiovascular risk factors in end-stage renal disease. *J Am Soc Nephrol.* 2002;13:134–141.
8. Kumada M, Kihara S, Sumitsuji S, Kawamoto T, Matsumoto S, Ouchi N, Arita Y, Okamoto Y, Shimomura I, Hiraoka H, Nakamura T, Funahashi T, Matsuzawa Y. Association of hypoadiponectinemia with coronary artery disease in men. *Arterioscler Thromb Vasc Biol.* 2003;23:85–89.
9. Pischon T, Girman CJ, Hotamisligil GS, Rifai N, Hu FB, Rhimm EB. Plasma adiponectin levels and risk of myocardial infarction in men. *JAMA.* 2004;291:1730–1737.
10. Maeda N, Shimomura I, Kishida K, Nishizawa H, Matsuda M, Nagaretani H, Furuyama N, Kondo H, Takahashi M, Arita Y, Komuro R, Ouchi N, Kihara S, Tochino Y, Okutomi K, Horie M, Takeda S, Aoyama T, Funahashi T, Matsuzawa Y. Diet-induced insulin resistance in mice lacking adiponectin/ACRP30. *Nat Med.* 2002;8:731–737.
11. Yokota T, Oritani K, Takahashi I, Ishikawa J, Matsuyama A, Ouchi N, Kihara S, Funahashi T, Tenner AJ, Tomiyama Y, Matsuzawa Y. Adiponectin, a new member of the family of soluble defense collagens, negatively regulates the growth of myelomonocytic progenitors and the functions of macrophages. *Blood.* 2000;96:1723–1732.
12. Matsuda M, Shimomura I, Sata M, Arita Y, Nishida M, Maeda N, Kumada M, Okamoto Y, Nagaretani H, Nishizawa H, Kishida K, Komuro R, Ouchi N, Kihara S, Nagai R, Funahashi T. Role of adiponectin in preventing vascular stenosis. *J Biol Chem.* 2002;277:37487–37491.
13. Okamoto Y, Kihara S, Ouchi N, Nishida M, Arita Y, Kumada M, Ohashi K, Sakai N, Shimomura I, Kobayashi H, Terasaka N, Inaba T, Funahashi T, Matsuzawa Y. Adiponectin reduces atherosclerosis in apolipoprotein E-deficient mice. *Circulation.* 2002;106:2767–2770.
14. Kato H, Honda S, Yoshida H, Kashiwagi H, Shiraga M, Honma N, Kurata Y, Tomiyama Y. SHPS-1 negatively regulates integrin $\alpha_{IIb}\beta_3$ function through CD47 without disturbing FAK phosphorylation. *J Thromb Haemost.* 2005;3:763–774.
15. Sano T, Oda E, Yamashita T, Shiramasa H, Ijiri Y, Yamashita T, Yamamoto J. Antithrombotic and anti-atherogenic effects of partially defatted flaxseed meal using a laser-induced thrombosis test in apolipoprotein E and low-density lipoprotein receptor deficient mice. *Blood Coagul Fibrinolysis.* 2003;14:707–712.
16. Tsuji S, Sugimoto M, Miyata S, Kuwahara M, Kinoshita S, Yoshioka A. Real-time analysis of mural thrombus formation in various platelet aggregation disorders: distinct shear-dependent roles of platelet receptors and adhesive proteins under flow. *Blood.* 1999;94:968–975.
17. Ouchi N, Kobayashi H, Kihara S, Kumada M, Sato K, Inoue T, Funahashi T, Walsh K. Adiponectin stimulates angiogenesis by promoting cross-talk between AMP-activated protein kinase and Akt signaling in endothelial cells. *J Biol Chem.* 2004;279:1304–1309.
18. Tomiyama Y, Kashiwagi H, Kosugi S, Shiraga M, Kanayama Y, Kurata Y, Matsuzawa Y. Abnormal processing of the glycoprotein IIb transcript due to a nonsense mutation in exon 17 associated with Glanzmann's thrombasthenia. *Thromb Haemost.* 1995;73:756–762.
19. Yamauchi T, Kamon J, Ito Y, Tsuchida A, Yokomiza T, Kita S, Sugiyama T, Miyagishi M, Hara K, Tsunoda M, Murakami K, Ohteki T, Uchida S, Takekawa S, Waki H, Tsuno NH, Shibata Y, Terauchi Y, Froguel P, Tobe K, Koyasu S, Taira K, Kitamura T, Shimizu T, Nagai R, Kadowaki T. Cloning of adiponectin receptors that mediate antidiabetic metabolic effects. *Nature.* 2003;423:762–769.
20. Bluher M, Fasshauer M, Kralisch S, Schon MR, Krohn K, Paschke R. Regulation of adiponectin receptor R1 and R2 gene expression in adipocytes of C57BL/6 mice. *Biochem Biophys Res Commun.* 2005;329:1127–1132.
21. Kashiwagi H, Honda S, Tomiyama Y, Mizutani H, Take H, Honda Y, Kosugi S, Kanayama Y, Kurata Y, Matsuzawa Y. A novel polymorphism in glycoprotein IV (replacement of proline-90 by serine) predominates in subjects with platelet GPIV deficiency. *Thromb Haemost.* 1993;69:481–484.
22. Chinetti G, Zawadski C, Fruchart JC, Staels B. Expression of adiponectin receptors in human macrophages and regulation by agonists of the nuclear receptors PPARα, PPARγ, and LXR. *Biochem Biophys Res Commun.* 2004;314:151–158.
23. Okamoto Y, Arita Y, Nishida M, Muraguchi M, Ouchi N, Takahashi M, Igura T, Inui Y, Kihara S, Nakamura T, Yamashita S, Miyagawa J, Funahashi T, Matsuzawa Y. An adipocyte-derived plasma protein, adiponectin, adheres to injured vascular walls. *Horm Metab Res.* 2000;32:47–50.
24. Fuster V, Badimon L, Badimon JJ, Chesebro JH. The pathogenesis of coronary artery disease and the acute coronary syndromes. *N Engl J Med.* 1992;326:242–250.
25. Ouchi N, Kihara S, Funahashi T, Nakamura T, Nishida M, Kumada M, Okamoto Y, Ohashi K, Nagaretani H, Kishida K, Nishizawa H, Maeda N, Kobayashi H, Hiraoka H, Matsuzawa Y. Reciprocal association of C-reactive protein with adiponectin in blood stream and adipose tissue. *Circulation.* 2003;107:671–674.
26. Chen H, Montagnant M, Funahashi T, Shimomura I, Quon MJ. Adiponectin stimulates production of nitric oxide in vascular endothelial cells. *J Biol Chem.* 2003;278:45021–45026.
27. Meehan WP, Knitter GH, Lasser GW, Lewis K, Ulla MM, Bishop PD, Hanson SR, Fruebis J. C1q-TNF related protein-1 (CTRP1) prevents thrombus formation in non-human primates and atherosclerotic rabbits without causing bleeding. *Blood* 2002;100:23a.
28. Wang Y, Lam KS, Xu JY, Lu G, Xu LY, Cooper GJ, Xu A. Adiponectin inhibits cell proliferation by interacting with several growth factors in an oligomerization-dependent manner. *J Biol Chem.* 2005;280:18341–18347.
29. Leung LL. Role of thrombospondin in platelet aggregation. *J Clin Invest.* 1984;74:1764–1772.
30. Bonnefoy A, Hantgan R, Legrand C, Frojmovic MM. A model of platelet aggregation involving multiple interactions of thrombospondin-1, fibrinogen, and GPIIbIIIa receptor. *J Biol Chem.* 2001;276:5605–5612.

Journal of Thrombosis and Haemostasis, **4**: 1379–1387

ORIGINAL ARTICLE

Critical role of ADP interaction with $P2Y_{12}$ receptor in the maintenance of $\alpha_{IIb}\beta_3$ activation: association with Rap1B activation

T. KAMAE,*[1] M. SHIRAGA,*[1] H. KASHIWAGI,* H. KATO,* S. TADOKORO,* Y. KURATA,† Y. TOMIYAMA* and Y. KANAKURA*

**Department of Hematology and Oncology, Graduate School of Medicine C9, Osaka University; and †Department of Blood Transfusion, Osaka University Hospital, Osaka, Japan*

To cite this article: Kamae T, Shiraga M, Kashiwagi H, Kato H, Tadokoro S, Kurata Y, Tomiyama Y, Kanakura Y. Critical role of ADP interaction with $P2Y_{12}$ receptor in the maintenance of $\alpha_{IIb}\beta_3$ activation: association with Rap1B activation. *J Thromb Haemost* 2006; **4**: 1379–87

Summary. *Objective:* Platelet integrin $\alpha_{IIb}\beta_3$ plays a crucial role in platelet aggregation, and the affinity of $\alpha_{IIb}\beta_3$ for fibrinogen is dynamically regulated. Employing modified ligand-binding assays, we analyzed the mechanism by which $\alpha_{IIb}\beta_3$ maintains its high-affinity state. *Methods and results:* Washed platelets adjusted to 50×10^3 μL^{-1} were stimulated with 0.2 U mL^{-1} thrombin or 5 μM U46619 under static conditions. After the completion of $\alpha_{IIb}\beta_3$ activation and granule secretion, different kinds of antagonists were added to the activated platelets. The activated $\alpha_{IIb}\beta_3$ was then detected by fluorescein isothiocyanate (FITC)-labeled PAC1. The addition of 1 μM AR-C69931MX (a $P2Y_{12}$ antagonist) or 1 mM A3P5P (a $P2Y_1$ antagonist) disrupted the sustained $\alpha_{IIb}\beta_3$ activation by ~92% and ~38%, respectively, without inhibiting CD62P or CD63 expression. Dilution of the platelet preparation to 500 μL^{-1} also disrupted the sustained $\alpha_{IIb}\beta_3$ activation, and the disruption by such dilution was abrogated by the addition of exogenous adenosine 5′-diphosphate (ADP) in a dose-dependent fashion. The amounts of ADP released from activated platelets determined by high-performance liquid chromatography were compatible with the amounts of exogenous ADP required for the restoration. We next examined the effects of antagonists on protein kinase C (PKC) and Rap1B activation induced by 0.2 U mL^{-1} thrombin. Thrombin induced long-lasting PKC and Rap1B activation. AR-C69931MX markedly inhibited Rap1B activation without inhibiting PKC activation. *Conclusions:* Our data indicate that the continuous interaction between released ADP and $P2Y_{12}$ is critical for the maintenance of $\alpha_{IIb}\beta_3$ activation.

Keywords: $\alpha_{IIb}\beta_3$ activation, adenosine 5′-diphosphate, $P2Y_{12}$, protein kinase C, Rap 1B.

Introduction

Platelet $\alpha_{IIb}\beta_3$ (GPIIb-IIIa), a non-covalently associated heterodimer, is a prototypic integrin that functions as a physiologic receptor for fibrinogen and von Willebrand factor (VWF). $\alpha_{IIb}\beta_3$ plays a crucial role in platelet aggregation, a key event of hemostatic plug formation and pathologic thrombus formation [1–3]. Inherited abnormalities in the expression or the function of $\alpha_{IIb}\beta_3$ preclude platelet aggregation, resulting in the bleeding disorder Glanzmann thrombasthenia (GT) [4,5]. Conversely, clinical studies have shown the beneficial effects of $\alpha_{IIb}\beta_3$ antagonists in patients undergoing coronary angioplasty or suffering from unstable angina [6,7]. During thrombogenesis, the affinity of $\alpha_{IIb}\beta_3$ for macromolecular ligands is dynamically regulated [1–3]. In resting platelets, $\alpha_{IIb}\beta_3$ is in a low-affinity state and does not bind soluble macromolecular ligands. However, after exposure to the subendothelial matrix, several mediators such as adenosine 5′-diphosphate (ADP) and thromboxane A_2, or shear stress, platelets become activated and activation signals (inside-out signaling) that induce a high-affinity state of $\alpha_{IIb}\beta_3$ for soluble ligands ($\alpha_{IIb}\beta_3$ activation) are generated. So far, much attention has been directed to the nature of inside-out signaling, and major advances have recently been made regarding the structural basis of $\alpha_{IIb}\beta_3$ activation, resulting in the proposal of 'switchblade' and 'deadbolt' models [8,9].

Previous studies revealed that the activation of $\alpha_{IIb}\beta_3$ is a reversible process [10,11]. When platelets are stimulated with weak agonists such as ADP in the absence of fibrinogen, $\alpha_{IIb}\beta_3$ gradually loses its binding capacity. In contrast,

Correspondence: Yoshiaki Tomiyama, Department of Hematology and Oncology, Graduate School of Medicine C9, Osaka University, 2-2 Yamadaoka, Suita Osaka 565-0871, Japan.
Tel.: +81 6 6879 3732; fax: +81 6 6879 3739;
e-mail: yoshi@hp-blood.med.osaka-u.ac.jp

[1]These authors contributed equally to this work.

Received 5 December 2005, accepted 16 February 2006